Differential induction of interferon stimulated genes between type I and type III interferons is independent of interferon receptor abundance

Kalliopi Pervolaraki[1,2], Soheil Rastgou Talemi[3,4], Dorothee Albrecht[1], Felix Bormann[5], Connor Bamford[6], Juan Mendoza[7], Christopher Garcia[7] , John McLauchlan[6], Thomas Höfer[3,4], Megan L. Stanifer[1,¶] , Steeve Boulant[1,2,¶,*]

[1] Schaller research group at CellNetworks, Department of Infectious Diseases, Virology, Heidelberg University Hospital, Heidelberg, Germany

[2] Division of Cellular polarity and viral infection, German Cancer Research Center (DKFZ), Heidelberg, Germany

[3]Division of Theoretical Systems Biology, German Cancer Research Center (DKFZ), Heidelberg, Germany

[4]BioQuant Center, Heidelberg University, Heidelberg, Germany

[5] Division of Epigenetics, German Cancer Research Center (DKFZ), Heidelberg, Germany

[6]MRC- University of Glasgow Centre for Virus Research, Glasgow, United Kingdom

[7]Howard Hughes Medical Institute, Department of Molecular and Cellular Physiology and Department of Structural Biology, Standford University School of Medicine, Standford, CA, United States of America

[*]Corresponding author: e-mail: s.boulant@dkfz.de (SB)

[¶] These authors contributed equally to this work

Abstract

It is currently believed that type I and III interferons (IFNs) have redundant functions. However, the preferential distribution of type III IFN receptor on epithelial cells suggests functional differences at epithelial surfaces. Here, using human intestinal epithelial cells we could show that although both type I and type III IFNs confer an antiviral state to the cells, they do so with distinct kinetics. Type I IFN signaling is characterized by an acute strong induction of interferon stimulated genes (ISGs) and confers fast antiviral protection. On the contrary, the slow acting type III IFN mediated antiviral protection is characterized by a weaker induction of ISGs in a delayed manner compared to type I IFN. Moreover, while transcript profiling revealed that both IFNs induced a similar set of ISGs, their temporal expression strictly depended on the IFNs, thereby leading to unique antiviral environments. Using a combination of data-driven mathematical modeling and experimental validation, we addressed the molecular reason for this differential kinetic of ISG expression. We could demonstrate that these kinetic differences are intrinsic to each signaling pathway and not due to different expression levels of the corresponding IFN receptors. We report that type III IFN is specifically tailored to act in specific cell types not only due to the restriction of its receptor but also by providing target cells with a distinct antiviral environment compared to type I IFN. We propose that this specific environment is key at surfaces that are often challenged with the extracellular environment.

Author summary

The human intestinal tract plays two important roles in the body: first it is responsible for nutrient absorption and second it is the primary barrier which protects the human body from the outside environment. This complex tissue is constantly exposed to commensal bacteria and is often exposed to both bacterial and viral pathogens. To protect itself, the gut produces, among others, secreted agents called interferons which help to fight against pathogen attacks. There are several varieties (type I, II, and III) of interferons and our work aims at understanding how type I and III interferon act to protect human intestinal epithelial cells (hIECs) during viral infection. In this study, we confirmed that both interferons can protect hIECs against viral infection but with different kinetics. We determined that type I confer an antiviral state to hIECs faster than type III interferons. We uncovered that these differences were intrinsic to each pathway and not the result of differential abundance of the respective interferon receptors. The results of this study suggest that type III interferon may provide a different antiviral environment to the epithelium target cells which is likely critical for maintaining gut homeostasis. Our findings will also help us to design therapies to aid in controlling and eliminating viral infections of the gut.

Introduction

During viral infection interferons (IFNs) are the predominant cytokines made to combat viral replication and spread. Following binding to specific receptors, IFNs induce a JAK/STAT signaling cascade which results in the production of interferon stimulated genes (ISGs). These ISGs will then establish an antiviral state within the cell and will also alert surrounding cells and immune cells to assist in viral clearance [1]. There are three classes of IFNs. Type I IFNs are produced by all cell types and are recognized by the ubiquitously expressed heterodimeric receptor IFNAR1/IFNAR2. Type II IFNs are only produced by immune cells [2,3]. Type III IFNs are made by all cell types but the IFNLR1 (or IL28Ra) subunit of the heterodimeric receptor IFNLR1/IL10Rβ is restricted to epithelial and barrier surfaces and to a subset of immune cells [4–9]. Despite the fact that type I and type III IFNs are structurally unrelated and engage different receptors, signaling downstream of both receptors exhibits a remarkable overlap and leads to the induction of a similar pool of ISGs. These observations originally led to the hypothesis that type I and III IFNs were functionally redundant.

This model has been challenged more and more in recent studies which highlight that the cell type specific compartmentalization of IFNLR1 provides type III IFNs a unique potential for targeting local infections at mucosal surfaces. For example, *in vivo* data on enteric virus infection of the murine gastrointestinal tract showed that responsiveness to type III IFN is necessary and sufficient to protect murine intestinal epithelial cells (IECs) against rotavirus and reovirus infection [10–12]. On the contrary, type I IFN

was necessary to protect against viral infection of cells in the lamina propria and against systemic spread [10,11]. Likewise, it was demonstrated that fecal shedding of norovirus was increased in IFNLR1-deficient, but not IFNAR1-deficient, mice, showing that type III IFN uniquely controls local norovirus infection in the gut [13,14]. Similarly, in the respiratory tract, type III IFNs are predominately produced upon infection with influenza A virus [15–19]. However, as infection progresses type I IFN comes into play to reinforce viral inhibition by inducing a pro-inflammatory response [20].

Differences in the antiviral activity conferred by both cytokines appear to be not only driven by the spatial restriction of their receptors but also by intrinsic subtle differences in signal transduction. It was demonstrated, in human hepatocytes and lung epithelial cells, that type I IFN confers a more potent antiviral protection compared to type III IFNs [5,21–23]. Additionally, it was shown in human IECs that type III IFN partially requires MAP kinase activation to promote an antiviral state while type I IFN was independent of it [24]. Although it has been reported in many studies that very similar ISGs are induced upon type I or type III IFN stimulation of cells, work mostly performed in hepatocytes revealed that both cytokines induce these ISGs with different kinetics [21,25–27]. Type III IFN mediated signaling was found to be associated with a delayed and reduced induction of ISGs compared to type I IFNs [25,26]. Similar differences in the magnitude and/or kinetics of ISGs induction upon type I versus type III IFN treatment were observed in human primary keratinocytes, airway epithelial cells and in Burkitt's lymphoma derived B (Raji) cells, as well as in murine intestinal and lung epithelial cells and immune cells [20,28–31].

The molecular mechanisms leading to this delayed and reduced induction of ISGs upon type III IFN treatment remains unclear. As these differences in kinetics of ISG expression between both IFNs could not be directly explained by their signaling cascades an alternative explanation was proposed where type III IFN receptor is expressed at lower levels at the cell surface. This lower receptor expression level could provide a biochemical explanation for the observed differences in delayed kinetics and weaker amplitude of ISG expression compared to type I IFN. However, to date, there is no direct experimental evidence for this model. Similarly, whether the observed differences between both IFNs is intrinsic to both specific signal transduction pathways and whether it is restricted to some cell types (e.g. hepatocytes) or represents a global signaling signature in all cells expressing both IFN receptors has not been fully addressed.

In this study, we have investigated how type I and III IFNs establish their antiviral program in human mini-gut organoids and human IEC lines. We found that type I IFN can protect human IECs against viral infection faster than its type III IFN counterpart. Correspondingly, we determined that type I IFN displays both a greater magnitude and faster kinetics of ISG induction compared to the milder, slower type III IFN. By developing mathematical models describing both type I and type III IFN mediated production of ISGs and by using functional receptor overexpression approaches, we demonstrated that the observed lower magnitude of ISG expression for type III IFNs was partially the result of its lower receptor expression level compared to the type I IFN receptor. Inversely, the observed delayed kinetics of type III IFN cannot be explained by receptor expression level indicating that this

144 property is specific to type III IFN and inherent to its signaling pathway. Our
145 results highlight important differences existing between both type I and type III
146 IFN-mediated antiviral activity and ISG expression which are not only the
147 result of receptor compartmentalization but also through intrinsic fundamental
148 differences in each IFN-mediated signaling pathway.
149

150 ## Results

151 **Type III IFN-mediated antiviral protection is delayed compared to type I**
152 **IFN.**

153 We have previously reported that both type I and III IFNs mediate
154 antiviral protection in human IECs [24]. To address whether type I and type III
155 IFN have a different profile of antiviral activity in primary non-transformed
156 human IECs, as reported in human lung cells [22], we compared the antiviral
157 potency of both IFNs in human mini-gut organoids. Colon organoids were pre-
158 treated with increasing concentrations of either type I or III IFNs for 2.5 hours
159 and subsequently infected with vesicular stomatitis virus expressing luciferase
160 (VSV-Luc). Viral infection was assayed by bioluminescence and results
161 showed that both IFNs induced an antiviral state in a dose-dependent
162 manner. We observed that type I IFN was slightly more potent in protecting
163 against viral infection at higher concentration compare to type III IFNs. Type I
164 IFN could almost fully inhibit viral infection while type III IFN was only able to
165 reduce infection to around 80% (Fig 1A). Interestingly, the concentration of
166 type I IFN necessary to provide 90% of relative antiviral protection (EC90)
167 was significantly lower than the one for type III IFN (Fig 1B).

To determine whether type III IFN requires a prolonged treatment to achieve similar antiviral protection as observed with type I IFN, we performed a time course experiment in which human colon organoids were pre-treated for different times with either IFN prior infection with VSV-Luc (Fig 1C). We found that approximately 2 hours pre-treatment with type I IFN was sufficient to reduce VSV infection by 90% (10% remaining infection), while type III IFN required around 5 hours to achieve a 90% reduction of infectivity (Fig 1C and 1D). Interestingly, 24 hours of pretreatment was necessary for type III IFN to almost completely prevent VSV infection (Fig 1C). These results strongly suggest that both type I and type III IFN could have similar potency but that type III IFN requires more time to establish an antiviral state.

We next addressed how long after infection IFN treatment is still able to promote antiviral protection. Colon organoids were infected with VSV-Luc and treated at different times post-infection with either type I or III IFNs. Interestingly, type I IFN could inhibit viral replication even when added several hours post-infection. In contrast, type III IFN appeared to require a much longer time to establish its antiviral activity and was unable to efficiently protect the organoids after VSV infection has initiated (Fig 1E and 1F).

Importantly, these differences in the kinetics of antiviral activity of type I versus type III IFNs were neither donor nor colon specific as similar results were observed in intestinal ileum-derived organoids derived from different donors (Sup Fig 1). In addition, human colon carcinoma-derived cell lines T84 (Sup Fig 2) and SKCO15 (data not shown) fully phenocopy the difference in type I versus type III IFN antiviral activity generated by primary mini-gut

192 organoids. Taken together these results demonstrate that while both type I
193 and III IFNs can promote similar antiviral states into target cells, they do so
194 with distinct kinetics. The cytokine-induced antiviral state is promoted faster
195 by type I IFN compared to type III IFN.

196 **Type I and III IFNs induce different amplitudes and kinetics of ISG**
197 **expression.**

198 To understand how type I and type III IFNs promote an antiviral state in
199 primary IECs but with different kinetics, we analyzed the magnitude of ISG
200 expression over time upon IFN treatment. Colon organoids were treated with
201 increasing concentrations of either type I or type III IFN and the expression
202 levels of two representative ISGs (IFIT1 and Viperin) were assayed at
203 different times post-IFN treatment. Results revealed that type I IFN ultimately
204 leads to a significantly higher induction of both IFIT1 and Viperin compared to
205 type III IFN (Fig 2A and 2B). This difference in the magnitude of ISG
206 stimulation was independent of the duration of IFN treatment (Fig 2A and 2B).
207 To determine if this pattern of expression applies to other ISGs, we treated
208 colon organoids with either type I or type III IFN over a 24-hour time course,
209 and analyzed the mRNA levels of 132 different ISGs and transcription factors
210 involved in IFN signaling (see complete list of genes and corresponding
211 primers in Sup Table 1 and 2) (Fig 2C and 2D). Differential expression
212 analysis revealed that both type I and type III IFNs induce almost the same
213 set of ISGs and that most of the genes significantly induced by type III IFN
214 were also induced by type I IFN (Fig 2C). However, similar to IFIT1 and
215 Viperin (Fig 2A and 2B), we found that the magnitude of ISG expression was

greater for type I IFN compared to type III IFN (Fig 2D). Similar results were found in the immortalized colon carcinoma-derived T84 cells (Sup Fig 3A-C).

To address whether there is any correlation between the different antiviral protection kinetics conferred by type I and III IFNs (Fig 1) and the kinetics of ISG expression, we analyzed the temporal expression of ISGs upon IFN treatment of human colon organoids. Hierarchical clustering analysis of all ISGs up-regulated upon type I or type III IFN treatment defined four distinct expression profiles based on the time of their maximum induction (Fig 3A-C). Group 1 are ISGs whose expression peaks 3 hours post-IFN treatment. The expression of ISGs in group 2 and 3 peaks at 6 and 12 hours post-treatment, respectively. Group 4 corresponds to ISGs with a continuous increase in expression over time (Fig 3A and B). Under type I IFN treatment, ISGs were nearly equally distributed in all four expression groups (Fig 3A, 3C, and 3D). By contrast, although the same ISGs were induced by type III IFN, they almost all belong to the expression group 4, being expressed later after IFN treatment (Fig 3B-D). In line with the primary mini-gut organoids, T84 cells presented similar differences in the kinetics of ISGs expression (Sup Fig 3D). Importantly, cell polarization of human IECs did not impact the kinetics of ISG expression as similar results were obtained when comparing polarized vs. non-polarized T84 cells (data not shown).

We next wanted to control that our observed differences in the kinetics of ISGs expression induced by both cytokines were independent of IFN concentration. Colon organoids were treated with increasing amounts of type I or type III IFNs and the transcriptional up-regulation of representative ISGs

240 belonging to each of the expression profile groups (group 1-4) was measured
241 over time (Fig 4). Consistent with our previous results, the temporal
242 expression patterns of each representative ISGs were independent of the IFN
243 concentration and the ISG expression kinetic signature was specific to each
244 IFN (Fig 4). Complementarily, to address whether the observed differences
245 between type I and type III IFNs were not due to the lower affinity of type III
246 IFN for its receptor compared to type I IFN, we employed the high affinity
247 variant of type III IFN (H11-IFNλ3) [32] to monitor the kinetics of ISG
248 expression. Results show that cells treated with the higher affinity H11-IFNλ3
249 display a higher magnitude of ISG expression but their kinetics of expression
250 were unchanged (Sup Fig 4). Altogether, our results strongly suggest that
251 although both type I and type III IFNs induce a similar set of ISGs in hIECs,
252 type III IFN induces globally a lower amplitude and a delayed ISG expression
253 compared to type I IFN.

254 **Mathematical modeling shows that IFN receptor abundance modulates**
255 **the magnitude of ISG response while the type I and type III IFN specific**
256 **kinetic profiles are independent of receptor abundance**

257 Our data show remarkable differences in the magnitude and kinetics of ISGs
258 induced by type I versus type III IFN (Fig 2-3 and Sup Fig 3), and in the
259 subsequent induction of a differential antiviral state (Fig 1 and Sup Fig 1-2).
260 To investigate the mechanisms underlying these differences, we used data-
261 driven mathematical modeling and model selection. We considered three
262 mechanistic causes for the observed differential signaling: (1) Receptor
263 abundance (different number of IFNLR compared to IFNAR complexes); (2)

Receptor regulation (different rates of activation and/or inactivation of IFNLR compared to IFNAR complexes); (3) STAT activation (different rates of STAT activation by type I and type III IFNs). We devised corresponding mathematical models describing the dynamics of receptor activation and inactivation, STAT1/2 phosphorylation and STAT-dependent activation of ISG expression (Fig 5A). The models were implemented as systems of ordinary differential equations (Sup Table 3) and fitted to the time-resolved data for the prototypical ISG, Viperin, measured with different doses of type I or type III IFNs and with the high affinity H11-IFNλ3. We ranked the models according to the Akaike information criterion corrected for small sample size (AICc), which evaluates the goodness of fit and, at the same time, penalizes the number of fit parameters (for more details see Materials and Methods). Throughout, we allowed different receptor abundance, but this difference alone could not account for the different signaling dynamics (Fig 5B; model M_1 has negligible support by the data, as quantified by the small AICc weight, which is a weight of evidence for the respective model). Interestingly, in addition to receptor abundance, the best-fitting model (M_3) has also different rates of activation and inactivation of IFNLR and IFNAR complexes. However, alternative models with different rates of STAT activation and/or ISG expression have good performance (M_2 and M_4, respectively). Therefore, the modeling indicates that differential ISG activation by type I and type III IFNs is likely due to different abundance of the respective receptors and cell-intrinsic differences in how the signals from bound receptors are processed.

The best-fitting model (M_3) accounted for the dose-response and the different Viperin expression kinetics triggered by type I, type III and the high affinity

289 H11-IFNλ3 in T84 cells, group 3 and group 4 expression kinetics, respectively
290 (Fig 5C, D). The different kinetics of the IFN responses – fast and transient for
291 type I IFN vs slower and sustained for type III IFN – are predicted to be largely
292 due to receptor inactivation, which is faster for IFNAR than for IFNLR complex
293 (Sup Fig 5A-C). Interestingly, the model shows that at low IFN concentrations,
294 Viperin is induced almost equally by both IFNs whereas at higher
295 concentrations, type I IFN induces Viperin more strongly (Fig 5E). These
296 dose-dependent features agree with our experimental data (Sup Fig 3B, right
297 panel).

298 Next, we tested the pivotal impact of receptor expression on ISG
299 induction that was indicated by our model. Specifically, the model predicts that
300 an increase in IFNAR1 or IFNLR1 level will increase the amplitude of ISG
301 induction while preserving the specific kinetic profiles elicited by the two types
302 of IFNs (Sup Fig 5D-E). To experimentally validate the model predictions,
303 IFNAR1 and IFNLR1 were overexpressed in T84 cells. Overexpression of the
304 respective IFN receptor chain was confirmed by reverse quantitative PCR
305 (Sup Fig 6). To ensure the functionality of both IFN receptors, IFNAR1 or
306 IFNLR1 were expressed in our previously characterized knockout T84 cell
307 lines deficient for either the IFN alpha receptor 1 (IFNAR1-/-) or the IFN
308 lambda receptor 1 (IFNLR1-/-) (Sup Fig 7A and 7E) [24]. Our results show
309 that overexpression of IFNAR1 in our IFNAR1-/- T84 cells (IFNAR1-/-
310 +rIFNAR1) restores their antiviral activity, their ability to phosphorylate STAT1
311 and induce the production of the ISGs IFIT1 and Viperin in the presence of
312 type I IFN (Sup Fig 7B-D). Similarly, although IFNLR1-/- cells were insensitive
313 to type III IFN treatment, overexpression of IFNLR1 (IFNLR1-/-+rIFNLR1)

314 restored their antiviral activity, pSTAT1 and ISG induction after addition of
315 type III IFN (Sup Fig 7F-H). These results demonstrate the functionality of
316 both IFN receptors and validate our overexpression approach as a means to
317 increase IFNAR1 and IFNLR1 levels at the cell surface.

318 Wild-type T84 cells overexpressing type I IFN receptor (WT+rIFNAR1)
319 were treated with increasing concentrations of type I IFN. Our results showed
320 elevated levels of STAT1 phosphorylation and ISG induction in response to
321 stimulation with type I IFN compared to wild-type cells (Fig 6A-D). Importantly,
322 the response of T84 cells overexpressing type I IFN receptor to type III IFN
323 remained unchanged, indicating a selective enhancement of the type I IFN
324 signaling pathway. Similarly, overexpression of type III IFN receptor
325 (WT+rIFNLR1) shows a significant increase in phosphorylated STAT1 and
326 ISG expression compared to wild-type cells upon type III IFN stimulation,
327 while no difference was observed upon type I IFN treatment (Fig 6E-H).
328 Altogether, our experimental data are consistent with the modeling predictions
329 and confirm the crucial impact of surface receptor levels for regulating the
330 magnitude of type I and III IFN response.

331 We next addressed whether this increase of ISG expression in cells
332 overexpressing either the type I or type III IFN receptor was associated with
333 an improved antiviral activity. Wild-type T84 cells overexpressing type I IFN
334 receptor (WT+rIFNAR1) were treated with type I IFN at different time points
335 prior to infection with VSV-Luc virus and their antiviral activity was compared
336 to wild-type T84 cells. Our results showed that the potency and the kinetics of
337 the antiviral activity of cells overexpressing type I IFN receptor does not

present any significant change upon type I IFN treatment (Sup Fig 8A). Similarly, there is no difference in the antiviral activity when cells overexpressing type I IFN receptor were treated with type I IFN at different time points post-infection (Sup Fig8B). However, overexpression of type III IFN receptor (WT+rIFNLR1) shows a modest but significant enhancement in type III IFN antiviral potency in the earlier time points of pre-treatment (between 30 minutes and 2 hours) compared to wild-type cells upon type III IFN stimulation (Sup Fig 8G), while they responded similarly to wild-type cells upon type I IFN treatment (Sup Fig 8E). Consistent with this, cells overexpressing type III IFN receptor are more protected than wild-type cells when type III IFN was added post-infection for the early time points (Sup Fig 8H).

Finally, to experimentally validate the limited impact of the IFN receptors abundance on the kinetic profile of ISG expression, as predicted by the model (Sup Fig 5D-E), wild-type cells overexpressing either of the IFN receptors were treated with increasing doses of type I or type III IFNs and the expression of a representative ISG belonging to each of the expression profile groups (group 1-4, Fig 3) was analyzed over time (Fig 7A-D). The experimental data show that the amplitude of ISG expression was dependent on both the dose of IFNs used to stimulate the cells and on the expression levels of the IFN receptors (Fig 7A-D). Importantly, the kinetic profile of ISG expression was similar between WT cells and cells overexpressing the IFNAR1 (WT+rIFNAR1), independent of the applied IFN type I dose (Fig 7A-D left panel). Similarly, wild-type cells overexpressing the IFNLR1 (WT+rIFNLR1) showed no change in the kinetic profile of ISG induction upon

type III IFN stimulation (Fig 7A-D right panel). Moreover, we found that the model reproduced the kinetic dose-response data when the IFNAR1 and IFNLR1 expression levels were increased ~2.6 and ~1.5 times, respectively, while all other parameters were held constant (Sup Fig 9). Indeed, we found that IFNAR1 overexpression was stronger than IFNLR1 overexpression, as judged by the transcript levels (Sup Fig 6B-C), with the ratio being consistent with the model prediction (Sup Fig 9D and Sup Fig 6B-C).

To directly correlate ISG expression kinetics and amplitude with the expression level of the type III IFN receptor, we thought of overexpressing an IFNLR1 tagged with the GFP fluorescent protein (IFNLR-GFP) in human IECs. To control the functionality of the GFP tagged receptor, the IFNLR1-GFP construct was overexpressed in the human embryonic kidney cell line 293 HEK, which normally elicit a very limited response upon type III IFN treatment. Quantitative RT-PCR revealed that 293 HEK cells overexpressing IFNLR1-GFP produced significantly more ISGs upon type III IFN treatment compared to WT 293 HEK cells or 293 HEK cells expression GFP alone (data not shown). Wild-type T84 cells overexpressing the IFNLR1-GFP (WT+rIFNLR1-GFP) were treated with type III IFN over time and cells were sorted by flow cytometry based on their level of IFNLR1-GFP expression (no GFP expressing (neg), or low and high GFP expressing cells) (Fig 8A). The induction of a representative ISG belonging to each of the expression profile groups (group 1-4, Fig 3) was measured over time in each sorted population (negative, low and high, Fig 8B). As anticipated, WT cells overexpressing the IFNLR1-GFP chain show stronger ISG expression compared to WT cells and the magnitude of the ISG induction correlates with the relative levels of

388 IFNLR1 expression (Fig 8B). However, the kinetic profiles of the ISGs upon
389 type III IFN stimulation were not affected by the differential expression levels
390 of the IFNLR1 chain (Fig 8B).

391 Altogether, our results demonstrate that type I and type III IFNs both
392 induce an antiviral state in hIECs but with different kinetics. We could show
393 that although both cytokines induce similar ISGs, type III IFN does it with
394 slower kinetics and lower amplitude of individual ISG expression compared to
395 type I IFN. Importantly, coupling mathematical modeling of both type I and
396 type III IFN-mediated signaling and overexpression of functional IFN receptors
397 approaches allowed us to demonstrate that these kinetic differences in type I
398 and type III IFN ISG expression are not due to different expression level of the
399 respective IFN receptors but are intrinsic to type I and type III IFN signaling
400 pathways.

Discussion

In this work, we have for the first time, performed a parallel study of the role of type I and III IFN in human mini-gut organoids and IEC lines. Our results demonstrate that type I and III IFNs are unique in their magnitude and kinetics of ISG induction. Type I IFN signaling is characterized by relatively strong expression of ISGs and confers to cells a fast-antiviral protection. On the contrary, the slow acting type III IFN mediated antiviral protection is characterized by a weak induction of ISGs in a delayed manner compared to type I IFN. Our results are in line with previous studies which also demonstrated that type III IFN is less potent than its type I IFN counterpart [5,21,23,33,34]. Additionally, we have confirmed that the delayed ISG induction seen upon type III IFN treatment of hepatocytes [21,23,25,26] is not tissue specific but likely represents a global pattern of action of this cytokine in cells expressing the type III IFN receptor (i.e. human epithelial cells). In other words, the different kinetics of ISG expression induced by type I and type III IFNs are specific to each IFN signaling pathways.

In the current work, we have employed, a data-driven mathematical modeling approach to explain signal transduction kinetic differences downstream type I and type III IFN receptors. While type I IFN-mediated signaling has been previously modeled [35,36], type III IFN has not. Our model predicted that the receptor levels directly influence the magnitude of ISG expression however, the kinetics of ISG expression appear to be intrinsic to each IFN-signaling pathway and is largely preserved under receptor overexpression. This prediction was experimentally validated by studying the

response of wild-type and IFN receptor overexpressing cells to different doses of IFN (Fig 7A-C and Fig 8). This suggests that the kinetic differences in the ISG induction are intrinsic to each IFN signaling pathway. We propose that these phenotypic differences reflect functional differences, which are important for mounting a well-tailored antiviral innate immune response at mucosal surfaces where type III IFN receptors are expressed.

Both type I and III IFNs have unique and independent receptors which are structurally unrelated. These receptors are likely expressed at different levels on individual cells and their relative expression to each other might also be cell type specific. To address whether the unique ISG and antiviral expression kinetics shown by each IFN were not due to differences in their expression levels, we overexpressed into cells functional type I (rIFNAR1) and type III IFN (rIFNLR1) receptors. Our results from IFNAR1 overexpressing cells (Fig 6 and 7) are in line with previous studies showing a direct relationship between the surface levels of type I IFN receptors and the magnitude of ISG induction [37,38]. Interestingly, we could demonstrate a similar relationship when overexpressing IFNLR1 (Fig 6 and 7) which was also associated with an increase of type III IFN antiviral potency (Sup Fig 8). These findings are in agreement with previous experiments which show that overexpression of IFNLR1 in cells which normally do not express this IFN receptor rescues both type III IFN-mediated signaling and IFN-mediated antiviral protection [5,28]. Our IFN receptor overexpression approach demonstrates that the observed differences in ISG expression kinetics are not the results of different levels of receptors at the cell surface but is likely specific to each signal transduction pathway. Apart from the expression levels

of IFN receptors, lower binding affinity towards their respective receptors could be an alternative explanation for the differential potencies of both type I and type III IFNs. Multiple studies have tried to affect the binding affinity of type I IFNs with their receptors however, results suggest that wild-type IFNs exert their antiviral activities already at maximum potency. Modifications leading to an increased affinity for their receptors do not lead to improvement of antiviral potency [32,38–41]. To address whether the weaker activity of type III IFN could be the result of its weaker affinity for its receptor, Mendoza et al, engineered a variant of type III IFN with higher-affinity for its receptor (H11-IFNλ3). They showed increased IFN signaling and antiviral activity in comparison with wild-type IFNλ3. However, the engineered variant of IFNλ3 was still acting with weaker efficacy compared to type I IFNs [32]. By exploiting the high affinity variant H11-IFNλ3, we could also show a significant increase of the amplitude of ISG expression but importantly, the kinetics of ISG expressions were not altered (Sup Fig 4).

Our results indicate a model were inherent temporal differences exist between type I and type III IFNs signaling. These differences are not the result of differential surface expression of the receptors but is the result of distinct signaling cascades from the receptors to the nucleus or within regulatory mechanisms of gene expressions.

While few studies have focused on the endocytosis and inactivation of IFNAR1, there is no information about how these processes occur for IFNLR1. It has been shown that the ternary IFNAR complex is internalized by clathrin mediated endocytosis [42] and that upon type I IFN stimulation,

IFNAR1 is rapidly endocytosed and routed for lysosomal degradation [43,44], whereas IFNAR2 can be recycled back to the cell surface or degraded [45]. Our data-driven mathematical modeling approach suggests a different kinetics of receptor activation/inactivation between both IFNs (Fig 5B and Sup Fig 5A). Therefore, further studies investigating trafficking of IFNLR1 will be important and may show that subtle changes in the time course of receptors internalization, recycling or degradation can have profound effect on kinetics of IFN activity. Apart from receptor internalization and degradation, several molecular mechanisms leading to IFN receptor inactivation have been described, such as de-phosphorylation [46,47], or by negatively targeting the interaction of IFNAR1 with downstream signaling elements of the JAK/STAT signaling, for instance ubiquitin-specific protease USP18, and members of the suppressor of cytokine signaling protein (SOCS) family. In particular, the inhibitory role of SOCS1 in type I IFN signaling has been demonstrated in a number of previous studies, where they have shown that SOCS1 associates with TyK2 and blocks its interaction with IFNAR1 [48]. USP18 has also been shown as an important negative regulator of type I IFN signaling with a dual role acting as isopeptidase which removes the ubiquitin like-ISG15 from target proteins [49] and as a competitor of JAK1 for binding to IFNAR2 [50]. Although, limited information is available for negative regulators of the IFNLR receptor complex, the specific contribution of USP18 or SOCS in inhibition of type I versus type III IFN mediated signaling has been addressed in recent studies. In particular, it has been showed that both type I and III IFNs (IFNα, IFNβ and IFNλ1, λ2, λ3 and λ4) induced the expression of USP18, SOCS1 and SOCS3 [51–57] and overexpression of all these negative regulators

inhibited both IFNα and IFNλ1 mediated JAK-STAT signaling [54,56] suggesting that at ‘’supraphysiological’’ expression levels all the inhibitors can block type I and type III mediated JAK-STAT signaling [56]. Additionally, it has been shown that USP18 is induced later and that its level increased over time, correlating with the long lasting refractories of IFNα signaling [51,52,56]. In our study we observed also a later peak of induction of USP18 at 12h or 24h upon type I or type III IFNs, respectively. In line with the above-mentioned studies we also observed rapid and transient induction of SOCS1 upon type I IFN treatment and sustained induction upon type III IFN stimulation. However, further investigation is required to determine the correlation of the kinetics of induction of these negative regulators with the ISGs induction in type I versus type III IFN treatment in human IECs.

In the canonical type I and III IFN signaling pathway the next downstream players from the IFN receptors are the JAKs, STAT1, STAT2 and IRF9, which are all regulated on the level of expression and activation. Our own observations (data not shown) and previous studies could not explain the major differences in the kinetics of type I versus type III IFNs activity by focusing on the time course of phosphorylation of STATs [21,25]. However, given that alternative modifications of STATs (*e.g.* phosphorylation on alternative residues, acetylation, methylation and sumoylation patterns) have been proposed to contribute to the activity of type I IFNs [26,58–60] it might be possible that new modifiers of STAT activity may determine the kinetic pattern of action of type I versus type III IFNs. In addition, apart from the JAK/STAT axis, there is accumulating evidence which correlates ISG transcription upon IFN treatment with a plethora of JAK-STAT independent

pathways, such as members of the CRK [61–63] and MAPKinase family [24,28,64–66], which might also temporally coordinate IFNs kinetic profile of action. Apart from the differences in the signaling cascade of type I versus type III IFNs, an explanation for their differential kinetics of action might stem from the physiology of the different cell types. For example, in a recent study Bhushal et al. reported that polarization of mouse intestinal epithelial cells eliminates the kinetic differences between type I and type III IFNs, by accelerating type III IFN responses [33,67].

Several studies describing the transcriptional activities of both type I and type III IFNs have reported that very similar sets of ISGs are produced upon both type I and III IFN stimulation [12,17,21,22,25,28] while only few ISGs appear to be predominantly expressed upon type III IFN treatment in murine IECs [67]. We believe that there are several functional advantages for adopting a lower and slower activity, like the profile of action of type III IFN, in the antiviral protection of epithelial tissues. The differences in the temporal expression of ISGs could create unique antiviral environments for each IFN. Many ISGs function as pro-inflammatory factors [30,68]. By stimulating ISGs production in high magnitude, an excessive amount of antiviral and pro-inflammatory signals could be produced which on the one hand will eliminate efficiently viral spreading but on the other hand may cause local exacerbated inflammation and irreversible tissue damage, leading to chronic inflammation in mucosal surfaces.

In addition, the expression of different functional groups of ISGs at early and at late time points (Fig 3) might allow cells to create two distinct

549 phases within the antiviral response. At early time points, minimum levels of
550 ISGs may act to protect the host against viral infection. Antiviral ISGs will be
551 responsible for fighting the pathogens and pro-inflammatory ISGs will
552 stimulate members of the adaptive immune system to assist the antiviral
553 protection. At later time points the produced ISGs, may be involved in anti-
554 inflammatory processes, such as resolving of inflammation and tissue healing
555 and repair [66,69]. To exert this anti-inflammatory role, ISGs may need to be
556 produced in higher levels, as they might act more paracrine and spread
557 through the tissue to balance again the tissue homeostasis after the viral
558 attack. In conclusion, we propose that type III IFN-mediated signaling is not
559 only set to act predominantly at epithelium surfaces due to the restriction of its
560 receptor but also is specifically tailored to mount a distinct immune state
561 compared to other IFNs which is critical for mucosal surfaces that face the
562 challenge.
563

564 ## Materials and Methods

565 ### Antibodies/Reagents

566 Commercially available primary antibodies were mouse monoclonal
567 antibodies recognizing beta-Actin (Sigma #A5441), phospho STAT1 and
568 STAT1 (BD Transductions #612233 and #610115, respectively). Anti-mouse
569 (GE Healthcare #NA934V), coupled with horseradish peroxidase was used as
570 secondary antibody for Western blot at a 1:5000 dilution. Human recombinant
571 IFN-beta1a (IFNβ) was obtained from Biomol (#86421). Recombinant human
572 IFNλ1 (IL-29) (#300-02L) and IFNλ2 (IL28A) (#300-2K) were purchased from
573 Peprotech and IFNλ3 (IL-28B) from Cell signaling (#8796). High affinity

574 engineered IFNλ3 variant (H11) and wild type IFNλ3 were produced as
575 described in [32] .The IFN concentrations used to treat the cells are stated in
576 the main text and in the figure legends.
577
578 **Cell and Viruses**
579 T84 human colon carcinoma cells (ATCC CCL-248) were maintained in a
580 50:50 mixture of Dulbecco's modified Eagle's medium (DMEM) and F12
581 (GibCo) supplemented with 10% fetal bovine serum and 1%
582 penicillin/streptomycin (GibCo). SKCO15 cells were maintained in DMEM with
583 10% fetal bovine serum, 1% penicillin/streptomycin, 15mM HEPES and 1%
584 NEAA (Non-Essential Amino Acids). Mini-gut organoids were harvested and
585 maintained as described earlier [24]. VSV-Luc was used as previously
586 described [24].
587
588 **Ethics Statement**
589 Human colon tissue was received from colon and small intestine resection
590 from the University Hospital Heidelberg. This study was carried out in
591 accordance with the recommendations of "University Hospital Heidelberg"
592 with written informed consent from all subjects. All subjects gave written
593 informed consent in accordance with the Declaration of Helsinki. All samples
594 were received and maintained in an anonymized manner. The protocol was
595 approved by the "Ethic commission of University Hospital Heidelberg" under
596 the approved study protocol S-443/2017.
597
598 **RNA isolation, cDNA, and qPCR**

RNA was harvested from cells using NucleoSpin RNA extraction kit (Macherey-Nagel) as per manufacturer's instructions. cDNA was made using iSCRIPT reverse transcriptase (BioRad) from 200ng of total RNA as per manufacturer's instructions. qRT-PCR was performed using SsoAdvanced SYBR green (BioRad) as per manufacturer's instructions, TBP and HPRT1 were used as normalizing genes.

Gene expression analysis of interferon stimulating genes

Colon organoids and T84 cells were treated with 2000 RU/ml of type I IFN (β) or 100 ng/ml of each type III IFN (λ1,2 and 3). Total RNA was isolated at 3, 6, 12 and 24h post-treatment as described above. For the gene expression analysis of interferon stimulated genes (ISGs), qRT-PCR was performed using the predesigned 384-well assay of type I IFN response for use with SYBR Green assaying the expression of 87 ISGs (Biorad # 10034592). The expression of 45 additional ISGs and transcriptional factors was analyzed by qRT-PCR with primer sets obtained as previously described [27]. The complete gene list monitored in this study and the primers used to amplify each gene is available in Tables S1 and S2. Differential expression analysis of each treatment was performed by comparing the baseline expression of genes in an untreated control at each time point. Only genes which were either induced or reduced more than 2-fold in any of the samples were considered to be significantly regulated. These genes were either analyzed using scatterplots or visualized by a heatmap after sorting the fold change of expression in response to type I IFN (β) in decreasing order. For the T84 cells all fold change values above 20 and below 0.05 were replaced with 20 and

624 0.05 respectively. For the organoids, the fold change values above 800 and
625 below 1/800 were replaced with 800 and 1/800. This data adaptation was
626 done to center the heatmap around 0 (white) and to avoid errors in logarithmic
627 calculations. When visualizing the expression peaks, only the highest value is
628 shown per time point for each gene. All analyses were performed using R
629 version 3.3.0 and 3.3.3 including the packages gplots and ggplot2.
630

631 **Western blot**

632 At time of harvest, media was removed, cells were rinsed one time with 1X
633 PBS and lysed with 1X RIPA buffer (150 mM sodium chloride, 1.0% Triton X-
634 100, 0.5% sodium deoxycholate, 0.1% sodium dodecyl sulphate (SDS), 50
635 mM Tris, pH 8.0 with phosphatase and protease inhibitors (Sigma-Aldrich)) for
636 20mins at 4°C. Lysates were collected and equal protein amounts were
637 separated by SDS-PAGE and blotted onto a PVDF membrane by wet-blotting.
638 Membranes were blocked with 5% milk or 5% BSA, when the phospho STAT1
639 antibody is used, in TBS containing 0.1% Tween 20 (TBS-T) for one hour at
640 room temperature. Primary antibodies were diluted in blocking buffer and
641 incubated overnight at 4°C. Membranes were washed 4X in TBS-T for 15mins
642 at RT. Secondary antibodies were diluted in blocking buffer and incubated at
643 RT for 1h with rocking. Membranes were washed 4X in TBS-T for 15mins at
644 RT. HRP detection reagent (GE Healthcare) was mixed 1:1 and incubated at
645 RT for 5mins. Membranes were exposed to film and developed.
646

647 **VSV luciferase assay**

Colon organoids and T84 cells were seeded in a white F-bottom 96-well plate. Samples were pre-treated prior to infection or treated post-infection as indicated with increasing concentrations of type I or type III IFNs. VSV-Luc was added to the wells and the infection was allowed to proceed for 8hrs. At the end of the infection, media was removed, samples were washed 1X with PBS and lysed with Cell Lysis Buffer (Promega) at RT for 20 mins. A 1:1 dilution of Steady Glo (Promega) and Lysis Buffer were added to the samples and incubated at RT for 15 mins. Luminescence was read using an Omega Luminometer.

FACS analysis

Fluorescence-activated cell sorting (FACS) was performed on FACSMelody™ Cell Sorter (BD Biosciences). DAPI was added for nuclear staining. Data were processed using FlowJo 10.0.5.

Cloning and generation of stable cell lines

Knockout of IFNAR1 and IFNLR1 in T84 cells were achieved by using the CRISPR/Cas9 system as described earlier [24]. For back-compensation of the IFN receptor KO cell lines and for generation of wild-type T84 cells overexpressing the IFNAR1 and IFNLR1, plasmids containing the cDNA of IFNAR1 and IFNLR1 were obtained from a gateway compatible ORF bank (pENTRY221-IFNAR1) and from GE Healthcare (pCR_XL_TOPO_IFNLR1, #MHS6278-213246004), respectively. The IFNLR1-GFP construct (pC1-HsIFNLR1-GFP) was generated using the following cloning strategy. A mammalian expression plasmid producing a N-terminal EGFP-tagged

674 extracellular domain of IFNLR1 (EGFP-IFNLR1) was generated as follows:
675 cDNA corresponding to this open reading from was generated synthetically
676 (GeneArt, Life Technologies) and subsequently sub-cloned directly into the
677 pC1 expression plasmid (Promega) backbone. Specifically, monomeric EGFP
678 was introduced between the signal peptide sequence and the remaining
679 glycoprotein flanked by three alanine residues at its amino terminus and a
680 short glycine-serine linker sequence of N-AAASGSGS-C at its carboxyl
681 terminus. Tri-alanine flanking allowed facile incorporation of restriction
682 enzyme sites (Not1 and SacII) allowing removal or swapping of EGFP tag.
683 Sequences available on request. Caspase-cleavage resistant IFNAR1 and
684 IFNLR1 were generated using the Quick Change II XL site directed
685 mutagenesis kit (Agilent Technologies, Germany), following manufacturer's
686 instructions. Point mutations were controlled by plasmid sequencing. The
687 expression vectors were generated by inserting the respective constructs into
688 the lentiviral vector pDest GW35 by using the Gateway cloning technology
689 (Life Technologies, Germany) according to manufacturer's instructions.
690 Lentiviruses were produced as previously described [24], and T84 cells were
691 transduced two times using concentrated stocks of lentiviral particles
692 encoding the cleavage resistant IFNAR1 and IFNLR1. 36 hours post-
693 transduction, transduced cells were selected for using blasticidin.
694
695 **Model simulation and parameter estimation**
696 The mathematical model was implemented in terms of ordinary differential
697 equations (ODEs) in MATLAB 2016b (S3 Table). The numerical simulations
698 were conducted using the CVODES, a module from SUNDIALS numerical

699 simulation package, in the MATLB environment. The model was initially set to
700 a steady state condition and most of the initial conditions were set (S4 Table).
701 Only, the IFNLR efficacy factor was estimated using time-resolved ISG
702 expression data that we measured with different doses of type I IFN (β) or III
703 IFN (λ1−3). All of the ISG expression data for the IFNAR1 and IFNLR1
704 overexpression experiments were reproduced only by fitting new initial values
705 of IFNAR1 and IFNLR1 (S5 Table).
706 Parameter estimation was conducted by minimizing the weighted nonlinear
707 least squares,

708 $$\mathrm{wSSR} = \sum_{i=1}^{N}\left(\frac{1}{Average(y_{observed\_i})}\right)\sum_{j=1}^{M}(y_{simulation\_i,j} - y_{observed\_i,j})^2,$$

709 of model simulations versus data points, j = 1, … , M, of different experiments,
710 i = 1, … , N. The inverse of the average of every time-resolved experimental
711 data was used as a weighting factor for fitting the corresponding data.
712
713
714 **Profile-likelihood analysis**
715 To assess the uncertainty in the estimated parameter values, we used the
716 profile-likelihood method [70]. In this method, the parameter confidence
717 bounds are calculated based on their contribution to the likelihoods, or in
718 another word, the objective function (wSSR). This computational approach is
719 conducted in a stepwise manner. In every step, the respective parameter is
720 fixed at a new value distant from the optimum estimated one. Then, the new
721 maximum likelihood is calculated ($\mathrm{wSSR}_{\min}(\theta)$). Using this approach, we can

calculate the profile of the maximum likelihoods over different values of the considered parameter. Then a threshold, Δ_α,

$$\Delta\chi^2 = \mathrm{wSSR}_{\min}(\theta) - \mathrm{wSSR}_{\min}(\theta_{\mathrm{optimum}}),$$
$$\{\theta \mid \Delta\chi^2 < \Delta_\alpha\},$$

is used to define the confidence bounds for the respective parameter. The threshold, Δ_α, is the α quantile of the chi-squared distribution.

Approximate 95% confidence bands calculation

To investigate the effect of the parameter uncertainty on model predictions we calculated approximate 95% confidence bands, as explained in Seber and Wild [71].

$$\text{Approx 95\% confidence bands} = y_{\text{simulated}} \pm t_{\text{invN}-P}^{\alpha} \cdot \sqrt{\text{MSE}} \cdot \left(1 + S \cdot (S \cdot S)^{-1} \cdot S\right)^{\frac{1}{2}}$$

where "$t_{\text{invN}-P}^{\alpha}$" is the α quantile of student's t distribution, "N" is the number of data points and "P" is the number of estimated model parameters, "MSE" is the mean standard error and "S" is the sensitivity matrix of the respective simulated observable.

Model selection

To select the most parsimonious model, the simplest model with good predictive power, from the ensemble of the four alternative models of the ISG

response to type I versus type III interferon, we used the Akaike information criterion corrected for small sample size (AICc). After fitting the models to the experimental data, we calculate the AICc score for every model. AICc is calculated as:

$$AICc = n\left(ln\left(\frac{2\pi \cdot wSSR}{n}\right) + 1\right) + 2k + \frac{2k(k+1)}{n-k-1},$$

where n is the number of data points used to fit the model, k is the number of estimated parameters of the respective model, and wSSR is the minimum weighted sum of squared residuals for the respective model. The model with the minimum AICc value is selected as the most parsimonious model from the ensemble of alternative models. In order to compare the selected model with other models, we calculate both ΔAICc, the difference between the AICc value of the models with the minimum AICc value from the ensemble of the models, and the AICc weight (w i). The Akaike weight is a weight of evidence for the respective model and is calculated as:

$$w_{\mathrm{i}} = \frac{exp\left(-\frac{1}{2}\Delta AICc_i\right)}{\sum_{r=1}^{M} exp\left(-\frac{1}{2}\Delta AICc_r\right)}.$$

Acknowledgments

We are grateful to the following colleagues for providing reagents Ronald L. Rabin and Lynnsey A. Renn (Center for Biologics Evaluation and Research, US Food and Drug Administration, USA) for the transcription factor primers, Sean Whelan (Harvard Medical School, USA) for the VSV-Luc and Asma Nusrat (University of Michigan, USA) for the SKCO15 cells. We would like to thank the members of Steeve Boulant Lab (Heidelberg University

Hospital, Germany) for their insights and helpful discussions in preparing the manuscript. We would like to thank the FACS facility at the EMBL, Heidelberg for their assistance in sorting the INFLR-GFP expressing cells.

References

1. Takeuchi O, Akira S. Innate immunity to virus infection. 2009;227:75–86.
2. Kawai T, Akira S. Innate immune recognition of viral infection. Nat Immunol. 2006;7(2):131–7.
3. Koyama S, Ishii KJ, Coban C, Akira S. Innate immune response to viral infection. Cytokine. 2008;43(3):336–41.
4. Kotenko S V, Gallagher G, Baurin V V, Lewis-Antes A, Shen M, Shah NK, et al. IFN-lambdas mediate antiviral protection through a distinct class II cytokine receptor complex. Nat Immunol. 2003;4(1):69–77.
5. Sheppard P, Kindsvogel W, Xu W, Henderson K, Schlutsmeyer S, Whitmore TE, et al. IL-28, IL-29 and their class II cytokine receptor IL-28R. Nat Immunol. 2003;4(1):63–8.
6. Sommereyns C, Paul S, Staeheli P, Michiels T. IFN-lambda (IFN-??) is expressed in a tissue-dependent fashion and primarily acts on epithelial cells in vivo. PLoS Pathog. 2008;4(3):1–12.
7. Mordstein M, Neugebauer E, Ditt V, Jessen B, Rieger T, Falcone V, et al. Lambda interferon renders epithelial cells of the respiratory and gastrointestinal tracts resistant to viral infections. J Virol. 2010;84(11):5670–7.
8. Donnelly RP, Kotenko S V. Interferon-lambda: a new addition to an old

family. J Interferon Cytokine Res. 2010;30(8):555–64.

9. Durbin RK, Kotenko S V., Durbin JE. Interferon induction and function at the mucosal surface. Immunol Rev. 2013;255(1):25–39.

10. Pott J, Mahlakõiv T, Mordstein M, Duerr CU, Michiels T, Stockinger S, et al. IFN-lambda determines the intestinal epithelial antiviral host defense. Proc Natl Acad Sci U S A. 2011;108(19):7944–9.

11. Mahlakõiv T, Hernandez P, Gronke K, Diefenbach A, Staeheli P. Leukocyte-Derived IFN-α/β and Epithelial IFN-λ Constitute a Compartmentalized Mucosal Defense System that Restricts Enteric Virus Infections. PLoS Pathog. 2015;11(4):1–19.

12. Lin J Da, Feng N, Sen A, Balan M, Tseng HC, McElrath C, et al. Distinct Roles of Type I and Type III Interferons in Intestinal Immunity to Homologous and Heterologous Rotavirus Infections. PLoS Pathog. 2016;12(4):1–29.

13. Baldridge MT, Nice TJ, McCune BT, Yokoyama CC, Kambal A, Wheadon M, et al. Commensal microbes and interferon-lambda determine persistence of enteric murine norovirus infection_supplemental data. Science. 2014;3(November):1–9.

14. Nice TJ, Baldridge MT, McCune BT, Norman JM, Lazear HM, Artyomov M, et al. Interferon-λ cures persistent murine norovirus infection in the absence of adaptive immunity. Science (80-). 2015;347(6219):269–73.

15. Contoli M, Message SD, Laza-Stanca V, Edwards MR, Wark P a B, Bartlett NW, et al. Role of deficient type III interferon-lambda production in asthma exacerbations. Nat Med. 2006;12(9):1023–6.

16. Baños-Lara MDR, Harvey L, Mendoza A, Simms D, Chouljenko VN,

820 Wakamatsu N, et al. Impact and regulation of lambda interferon
821 response in human metapneumovirus infection. J Virol.
822 2015;89(1):730–42.
823 17. Crotta S, Davidson S, Mahlakoiv T, Desmet CJ, Buckwalter MR, Albert
824 ML, et al. Type I and Type III Interferons Drive Redundant Amplification
825 Loops to Induce a Transcriptional Signature in Influenza-Infected Airway
826 Epithelia. PLoS Pathog. 2013;9(11).
827 18. Jewell N a, Cline T, Mertz SE, Smirnov S V, Flano E, Schindler C, et al.
828 Interferon-{lambda} is the predominant interferon induced by influenza A
829 virus infection in vivo. J Virol. 2010;84(21):11515–22.
830 19. Ank N, Iversen MB, Bartholdy C, Staeheli P, Hartmann R, Jensen UB,
831 et al. An Important Role for Type III Interferon (IFN- /IL-28) in TLR-
832 Induced Antiviral Activity. J Immunol. 2008;180(4):2474–85.
833 20. Galani IE, Triantafyllia V, Eleminiadou EE, Koltsida O, Stavropoulos A,
834 Manioudaki M, et al. Interferon-λ Mediates Non-redundant Front-Line
835 Antiviral Protection against Influenza Virus Infection without
836 Compromising Host Fitness. Immunity. 2017;46(5):875–890.e6.
837 21. Marcello T, Grakoui A, Barba-Spaeth G, Machlin ES, Kotenko S V.,
838 Macdonald MR, et al. Interferons ?? and ?? Inhibit Hepatitis C Virus
839 Replication With Distinct Signal Transduction and Gene Regulation
840 Kinetics. Gastroenterology. 2006;131(6):1887–98.
841 22. Voigt E a., Yin J. Kinetic Differences and Synergistic Antiviral Effects
842 Between Type I and Type III Interferon Signaling Indicate Pathway
843 Independence. J Interf Cytokine Res. 2015;0(0):150504080007003.
844 23. Kohli A, Zhang X, Yang J, Russell RS, Donnelly RP, Sheikh F, et al.

Distinct and overlapping genomic profiles and antiviral effects of Interferon-lambda and -alpha on HCV-infected and noninfected hepatoma cells. J Viral Hepat. 2012 Dec;19(12):843–53.

24. Pervolaraki K, Stanifer ML, Münchau S, Renn LA, Albrecht D, Kurzhals S, et al. Type I and type III interferons display different dependency on mitogen-activated protein kinases to mount an antiviral state in the human gut. Front Immunol. 2017;8(APR):1–16.

25. Jilg N, Lin W, Hong J, Schaefer E a., Wolski D, Meixong J, et al. Kinetic differences in the induction of interferon stimulated genes by interferon-α and interleukin 28B are altered by infection with hepatitis C virus. Hepatology. 2014;59(4):1250–61.

26. Bolen CR, Ding S, Robek MD, Kleinstein SH. Dynamic expression profiling of type I and type III interferon-stimulated hepatocytes reveals a stable hierarchy of gene expression. Hepatology. 2014;59(4):1262–72.

27. Novatt H, Theisen TC, Massie T, Massie T, Simonyan V. in Response to Interferon b and Interferon l 1. 2016;36(10):589–98.

28. Zhou Z, Hamming OJ, Ank N, Paludan SR, Nielsen AL, Hartmann R. Type III Interferon (IFN) Induces a Type I IFN-Like Response in a Restricted Subset of Cells through Signaling Pathways Involving both the Jak-STAT Pathway and the Mitogen-Activated Protein Kinases. J Virol. 2007;81(14):7749–58.

29. Alase AA, El-Sherbiny YM, Vital EM, Tobin DJ, Turner NA, Wittmann M. IFNλ stimulates MxA production in human dermal fibroblasts via a MAPK-dependent STAT1-independent mechanism. J Invest Dermatol.

2015;135(12):2935–43.

30. Davidson S, Mccabe TM, Crotta S, Gad HH, Hessel EM, Beinke S, et al. IFN k is a potent anti-influenza therapeutic without the inflammatory side effects of IFN a treatment. 2016;8(9):1099–112.

31. Broggi A, Tan Y, Granucci F, Zanoni I. IFN-λ suppresses intestinal inflammation by non-translational regulation of neutrophil function. Nat Immunol. 2017;18(10):1084–93.

32. Mendoza JL, Schneider WM, Hoffmann H, Jong YP De, Rice CM, Garcia KC, et al. The IFN- l -IFN- l R1-IL-10R b Complex Reveals Structural Features Underlying Type III IFN Functional Plasticity Article The IFN- l -IFN- l R1-IL-10R b Complex Reveals Structural Features Underlying. Immunity. 2017;46(3):379–92.

33. Bhushal S, Wolfsmüller M, Selvakumar TA, Kemper L. Cell Polarization and Epigenetic Status Shape the Heterogeneous Response to Type III Interferons in Intestinal Epithelial Cells. 2017;8(June).

34. Meager A, Visvalingam K, Dilger P, Bryan D, Wadhwa M. Biological activity of interleukins-28 and -29: Comparison with type I interferons. Cytokine. 2005;31(2):109–18.

35. Rand U, Rinas M, Werk JS, Nöhren G, Linnes M, Kröger A, et al. Multi-layered stochasticity and paracrine signal propagation shape the type-I interferon response. Mol Syst Biol. 2012;8(584):1–13.

36. Maiwald T, Schneider A, Busch H, Sahle S, Gretz N, Weiss TS, et al. Combining theoretical analysis and experimental data generation reveals IRF9 as a crucial factor for accelerating interferon-α induced early antiviral signalling. FEBS J. 2010;277(22):4741–54.

37. Moraga I, Harari D, Schreiber G, Uze G, Pellegrini S. Receptor Density Is Key to the Alpha2/Beta Interferon Differential Activities. Mol Cell Biol. 2009;29(17):4778–87.

38. Levin D, Harari D, Schreiber G. Stochastic Receptor Expression Determines Cell Fate upon Interferon Treatment. Mol Cell Biol. 2011;31(16):3252–66.

39. Kalie E, Jaitin DA, Abramovich R, Schreiber G. An interferon ??2 mutant optimized by phage display for IFNAR1 binding confers specifically enhanced antitumor activities. J Biol Chem. 2007;282(15):11602–11.

40. Kalie E, Jaitin DA, Podoplelova Y, Piehler J, Schreiber G. The stability of the ternary interferon-receptor complex rather than the affinity to the individual subunits dictates differential biological activities. J Biol Chem. 2008;283(47):32925–36.

41. Lavoie TB, Kalie E, Crisafulli-Cabatu S, Abramovich R, DiGioia G, Moolchan K, et al. Binding and activity of all human alpha interferon subtypes. Cytokine. 2011;56(2):282–9.

42. Suresh Kumar KG, Barriere H, Carbone CJ, Liu J, Swaminathan G, Xu P, et al. Site-specific ubiquitination exposes a linear motif to promote interferon-α receptor endocytosis. J Cell Biol. 2007;179(5):935–50.

43. Kumar KGS, Tang W, Ravindranath AK, Clark WA, Croze E, Fuchs SY. SCF HOS ubiquitin ligase mediates the ligand-induced down-regulation of the interferon- a receptor. 2003;22(20).

44. Marijanovic Z, Ragimbeau J, Kumar KGS, Fuchs SY, Pellegrini S. TYK2 activity promotes ligand-induced IFNAR1 proteolysis. Biochem J.

2006;397(1):31–8.

45. Weerd NA De, Samarajiwa SA, Hertzog PJ. Type I Interferon Receptors : Biochemistry and Biological. J Biol Chem. 2007;282(28):20053–7.

46. Myers MP, Andersen JN, Cheng A, Tremblay ML, Horvath CM, Parisien JP, et al. TYK2 and JAK2 Are Substrates of Protein-tyrosine Phosphatase 1B. J Biol Chem. 2001;276(51):47771–4.

47. Simoncic PD, Lee-loy A, Barber DL, Tremblay ML, Mcglade CJ. The T Cell Protein Tyrosine Phosphatase Is a Negative Regulator of Janus Family Kinases 1 and 3. Curr Biol. 2002;12(2):446–53.

48. Piganis RAR, De Weerd NA, Gould JA, Schindler CW, Mansell A, Nicholson SE, et al. Suppressor of Cytokine Signaling (SOCS) 1 inhibits type I interferon (IFN) signaling via the interferon α receptor (IFNAR1)-associated tyrosine kinase tyk2. J Biol Chem. 2011;286(39):33811–8.

49. Malakhov MP, Malakhova OA, Il Kim K, Ritchie KJ, Zhang DE. UBP43 (USP18) specifically removes ISG15 from conjugated proteins. J Biol Chem. 2002;277(12):9976–81.

50. Malakhova OA, Kim K Il, Luo J, Zou W, Suresh KG, Fuchs SY, et al. UBP43 is a novel regulator of interferon signaling independent of its ISG15 isopeptidase activity. EMBO J. 2006;25(11):2358–67.

51. Sarasin-Filipowicz M, Wang X, Yan M, Duong FHT, Poli V, Hilton DJ, et al. Alpha Interferon Induces Long-Lasting Refractoriness of JAK-STAT Signaling in the Mouse Liver through Induction of USP18/UBP43. Mol Cell Biol. 2009;29(17):4841–51.

52. François-Newton V, de Freitas Almeida GM, Payelle-Brogard B,

Monneron D, Pichard-Garcia L, Piehler J, et al. USP18-based negative feedback control is induced by type I and type III interferons and specifically inactivates interferon α response. PLoS One. 2011;6(7).

53. Makowska Z, Duong FHT, Trincucci G, Tough DF, Heim MH. Interferon-β and interferon-λ signaling is not affected by interferon-induced refractoriness to interferon-α in vivo. Hepatology. 2011;53(4):1171–80.

54. Liu B, Chen S, Guan Y, Chen L. Type III Interferon Induces Distinct SOCS1 Expression Pattern that Contributes to Delayed but Prolonged Activation of Jak/STAT Signaling Pathway: Implications for Treatment Non-Response in HCV Patients. PLoS One. 2015;10(7):e0133800.

55. Fan W, Xie S, Zhao X, Li N, Chang C, Li L, et al. IFN-λ4 desensitizes the response to IFN-α treatment in chronic hepatitis c through long-term induction of USP18. J Gen Virol. 2016;97(9):2210–20.

56. Blumer T, Coto-Llerena M, Duong FHT, Heim MH. SOCS1 is an inducible negative regulator of interferon λ (IFN-λ)-induced gene expression in vivo. J Biol Chem. 2017;292(43):17928–38.

57. Obajemu AA, Rao N, Dilley KA, Vargas JM, Sheikh F, Donnelly RP, et al. IFN-λ4 Attenuates Antiviral Responses by Enhancing Negative Regulation of IFN Signaling. J Immunol. 2017;ji1700807.

58. Uddin S, Sassano A, Deb DK, Verma A, Majchrzak B, Rahman A, et al. Protein kinase C-δ (PKC-δ) is activated by type I interferons and mediates phosphorylation of Stat1 on serine 727. J Biol Chem. 2002;277(17):14408–16.

59. Wieczorek M, Ginter T, Brand P, Heinzel T, Kra OH. Cytokine & Growth Factor Reviews Acetylation modulates the STAT signaling code.

2012;23:293–305.

60. Song L, Bhattacharya S, Yunus AA, Lima CD, Schindler C. Stat1 and SUMO modification. Blood. 2017;108(10):3237–45.

61. Platanias LC, Fish EN. Signaling pathways activated by interferons. Exp Hematol. 1999;27:1583–92.

62. Platanias LC. Mechanisms of type-I- and type-II-interferon-mediated signalling. Nat Rev Immunol. 2005;5(5):375–86.

63. Lekmine F, Sassano A, Uddin S, Majchrzak B, Miura O, Druker BJ, et al. The CrkL Adapter Protein Is Required for Type I Interferon-Dependent Gene Transcription and Activation of the Small G-Protein Rap1. Biochem Biophys Res Commun. 2002;750:744–50.

64. Uddin S, Majchrzak B, Woodson J, Arunkumar P, Alsayed Y, Pine R, et al. Activation of the p38 mitogen-activated protein kinase by type I interferons. J Biol Chem. 1999;274(42):30127–31.

65. Brand S, Beigel F, Olszak T, Zitzmann K, Eichhorst ST, Otte J-M, et al. IL-28A and IL-29 mediate antiproliferative and antiviral signals in intestinal epithelial cells and murine CMV infection increases colonic IL-28A expression. Am J Physiol Gastrointest Liver Physiol. 2005;289(5):G960–8.

66. Alase A a, El-Sherbiny YM, Vital EM, Tobin DJ, Turner N a, Wittmann M. IFNλ Stimulates MxA Production in Human Dermal Fibroblasts via a MAPK-Dependent STAT1-Independent Mechanism. J Invest Dermatol. 2015;(August):1–29.

67. Selvakumar TA, Bhushal S, Kalinke U, Wirth D, Hauser H, Köster M, et al. Identification of a predominantly interferon-λ-induced transcriptional

995 profile in murine intestinal epithelial cells. Front Immunol. 2017;8(OCT).
996 68. Andreakos E, Salagianni M, Galani IE, Koltsida O. Interferon-λs: Front-
997 line guardians of immunity and homeostasis in the respiratory tract.
998 Front Immunol. 2017;8(SEP):1–7.
999 69. Chiriac MT, Buchen B, Wandersee A, Hundorfean G, Günther C,
1000 Bourjau Y, et al. Activation of Epithelial Signal Transducer and Activator
1001 of Transcription 1 by Interleukin 28 Controls Mucosal Healing in Mice
1002 With Colitis and Is Increased in Mucosa of Patients With Inflammatory
1003 Bowel Disease. Gastroenterology. 2017;153(1):123–138.e8.
1004 70. Raue A, Kreutz C, Maiwald T, Bachmann J, Schilling M, Klingmüller U,
1005 et al. Structural and practical identifiability analysis of partially observed
1006 dynamical models by exploiting the profile likelihood. Bioinformatics.
1007 2009;25(15):1923–9.
1008 71. Seber GAF, Wild CJ. Nonlinear Regression. John Wiley & Sons.
1009 2003.775 p.

1010

1011 ## Figure Legends

1012 **Fig 1. Kinetics of type I and type III IFN-mediated antiviral activities in**
1013 **human mini gut-organoids.** (A-B) Colon organoids were pre-treated with the
1014 indicated concentrations of type I IFN (β) or type III IFN (λ1−3) for 2.5 h prior
1015 to infection with vesicular stomatitis virus (VSV) expressing Firefly luciferase
1016 (VSV-Luc) using a multiplicity of infection (MOI) of 1. Viral replication was
1017 assayed by measuring the luciferase activity. (A) The relative antiviral
1018 protection is expressed as a percentage of total protection in VSV-infected
1019 organoids or (B) as the EC90 corresponding to the concentration of type I IFN

(β) or type III IFN (λ1−3) resulting in 90% inhibition (10% infection) of viral replication. (C-D) Colon organoids were treated with type I IFN (β) (2,000 RU/mL equivalent 0.33 nM) or type III IFN (λ1−3) (100ng/mL each or total 300 ng/mL equivalent 13.7 nM) for different times prior to infection with VSV-Luc. Viral replication was assayed by measuring luciferase activity. (C) The relative VSV infection is expressed as the percentage of the luciferase activity present in VSV-infected organoids without IFN treatment (set to 100). (D) Pre-incubation time of type I IFN (β) or type III IFN (λ1−3) required to inhibit VSV infection to 10% (90% inhibition). (E-F) Same as (C-D), except colon organoids were treated at the indicated times post-infection with VSV-Luc. (F) Delayed-time post-infection for type I IFN (β) or type III IFN (λ1−3) to still inhibit VSV infection to 90% (10% inhibition). Data in (A–F) represent the mean values of two independent experiments. Error bars indicate the SD. *<P.05, **P < 0.01, ns, not significant (unpaired t-test).

Fig 2. Type III IFNs have a lower transcriptional activity compared to type I IFNs. (A-B) Human colon organoids were stimulated with indicated concentrations of type I (β) or III IFN (λ1−3) for different times and the transcript levels of the ISGs IFIT1 and Viperin were analyzed by qRT-PCR. Data are normalized to TBP and HPRT1 and are expressed relative to untreated samples at each time point. A representative experiment with technical triplicates, out of three independent experiments is shown. Mean values and SD are shown. (C) Colon organoids were treated with type I IFN (β) (2,000 RU/mL equivalent 0.33 nM) or type III IFN (λ1−3) (300 ng/mL equivalent 13.7 nM) for the indicated times and identification of the IFN-

1045 induced ISGs was performed by qRT-PCR. A total of 65 out of 132 ISGs
1046 tested were found to be significantly induced more than 2-fold compared with
1047 a baseline (mean of untreated controls at the particular time points) for at
1048 least one time point by at least one IFN treatment. Data are normalized to
1049 TBP and HPRT1 and visualized in a heatmap using R after sorting the fold
1050 change of expression in response to type I IFN (β) in decreasing order. (D)
1051 Comparison of expression values (log2 (Fold Change)) for all genes induced
1052 at the indicated times with type I IFN (β) versus type III IFN (λ1−3). Solid line
1053 indicates equivalent expression.
1054
1055 **Fig 3. Type III IFNs present delayed transcriptional activity compared to**
1056 **type I IFNs.** (A-D) Human colon organoids were treated with type I IFN (β)
1057 (2,000 RU/mL equivalent 0.33 nM) or type III IFN (λ1−3) (300 ng/mL
1058 equivalent 13.7 nM) for 3, 6, 12 or 24 hours and the kinetic pattern of
1059 expression of the 65 significantly up-regulated ISGs were analyzed by qRT-
1060 PCR in triplicates. Data are normalized to TBP and HPRT1 and are
1061 expressed relative to untreated cells at each time point. Hierarchical clustering
1062 analysis of these genes produced four distinct temporal expression patterns
1063 (Groups 1-4) based on the time-point of the maximum induction in response
1064 to type I IFN (β) or type III IFN (λ1−3). Color codes have been used to
1065 visualize the induction peak per group. (A-B) Gray lines show the normalized
1066 kinetic expression of each gene for each group upon treatment with (A) type I
1067 IFN (β) or (B) type III IFN (λ1−3). The colored lines are the average of the
1068 kinetic profiles for the genes of each group. (C) Gene expression heat map
1069 showing the genes clustered in their respective temporal expression patterns

groups in response to type I IFN (β) or type III IFN (λ1−3). The genes per group are sorted in decreasing order on the basis of their fold change of expression in response to type I IFN (β) or type III IFN (λ1−3) and only showing the highest expressed values within the temporal groups omitting all other values for visualization. (D) Number of genes belonging to each group.

Fig 4. Validation of the unique kinetic patterns of ISG expression upon type I versus type III IFN treatment. (A-D) Human colon organoids were stimulated with increasing concentrations of type I IFN (β) or III IFN (λ1−3) for indicated times and the kinetic pattern of expression of one representative ISG from each temporal expression patterns groups 1-4 was analyzed by qRT-PCR, (left column) type I IFN (β), (right column) type III IFN (λ1−3) treated organoids. Data are normalized to HPRT1 and are expressed relative to untreated cells at each time point. A representative experiment with technical triplicates. Mean values and SD are shown.

Fig 5. Mathematical modeling of type I and type III IFN responses. (A) Scheme of the mathematical model. IFNs bind to their cognate receptors and activate them; all molecules are also subject to degradation (∅). Active receptors mediate STAT phosphorylation while phosphorylated STAT (p-STAT) drives ISG expression. ISGs may include negative feedback regulator of STAT activation. Dashed lines indicate the potential sources of difference between the two pathways. Red dashed lines show the sources of the difference between the two pathways implemented in the best-fitting model. (B) Model selection. Models fitted to the experimental data were ranked using

the Akaike information criterion corrected for small sample size (AICc) and the AICc weight, as a measure of support for the given model by the data. (C-D) The best-fitting model M3 reproduces the Viperin expression dynamics upon treatment with different concentrations of (C) type I IFN and (D) type III IFN (see Sup Fig 3A-B for experimental data). In (C) and (D), the solid lines represent the best fits and the shaded areas are 95% confidence intervals. (E) Simulation of the maximum Viperin induction upon treatment with equal concentrations of type I IFN or type III IFN.

Fig 6. Overexpression of type I and type III IFN receptor increases the transcriptional activity of both cytokines. (A-F) Wild-type T84 cells were transduced with rIFNAR1 or rIFNLR1 to create stable lines overexpressing either IFN receptors. (A-B) T84 wild-type cells (WT) and T84 cells overexpressing rIFNAR1 (WT+rIFNAR1) were treated with type I IFN (β) (2,000 RU/mL equivalent 0.33 nM) or type III IFN (λ1−3) (300 ng/mL equivalent 13.7 nM) for 1h and IFN signaling was measured by immunoblotting for pSTAT1 Y701. Actin was used as a loading control. A representative immunoblot out of three independent experiments is shown. (C-D) T84 wild type cells (WT) and T84 cells overexpressing rIFNAR1 (WT+rIFNAR1) were treated with increasing concentrations of type I IFN (β) for 12 hours or type III IFN (λ1−3) for 24 hours and the transcript levels of the ISGs IFIT1 and VIPERIN were analyzed by qRT-PCR. Data are normalized to HPRT1 and are expressed relative to untreated cells at each time point. (E-H) Same as (A-D), except T84 cells overexpressing rIFNLR1 (WT+IFNLR1) were used. The mean value obtained from three independent experiments is

shown. Error bars indicate the SD. *<P.05, **P < 0.01, ***P < 0.001, ****P < 0.0001, ns, not significant (unpaired t-test).

Fig 7. Expression kinetics of ISGs are independent of the IFN receptor levels. (A-D) Wild-type T84 cells were transduced with rIFNAR1 or rIFNLR1 to create stable lines overexpressing either receptors. (blue panels) T84 wild-type cells (WT) and T84 cells overexpressing the IFNAR1 (WT+rIFNAR1) were treated with increasing concentrations of type I IFN (β) for the indicated times and the kinetic pattern of expression of one representative ISG from each temporal expression patterns groups 1-4 was analyzed by qRT-PCR. Data are normalized to HPRT1 and are expressed relative to untreated cells at each time point. (red panels) Same as (blue panels), except T84 cells overexpressing the IFNLR1 (WT+IFNLR1) were used and treated with increasing concentrations of type III IFN (λ1−3). A representative experiment with technical triplicates, out of three independent experiments is shown. Mean values and SD are shown.

Fig 8. Type III IFN mediated expression kinetics of ISGs are independent of differential levels of IFNLR1 receptor. Wild-type T84 cells were transduced with rIFNLR1-GFP to create a stable line overexpressing IFNLR1 tagged with GFP. (A) WT cells overexpressing IFNLR1-GFP (WT+IFNLR1-GFP) from the same population were separated by cell sorting into three populations: non (neg)-, low- and high-expressing GFP cells. Gates were created based on the auto-fluorescence of WT cells. (B) WT and WT+IFNLR1-GFP cells were treated with type III IFN (λ1−3) (300 ng/mL

equivalent 13.7 nM) for 3, 6, 12 and 24 hours prior to sorting in neg-, low- and high-expressing IFNLR1-GFP cells. The kinetic pattern of expression of one representative ISG from each temporal expression patterns groups 1-4 was analyzed by qRT-PCR in each sorted population. Data are normalized to HPRT1 and are expressed relative to untreated cells at each time point. A representative experiment with technical triplicates, out of two independent experiments is shown. Mean values and SD are shown.

Supporting Information Legends

Sup Fig 1. Kinetics of type I and type III IFN-mediated antiviral activities in intestinal organoids. (A-B) Intestinal organoids were pre-treated with the indicated concentrations of type I IFN (β) or type III IFN (λ1−3) for 2.5 h prior to infection with VSV-Luc using a multiplicity of infection (MOI) of 1. Viral replication was assayed by measuring the luciferase activity. (A) The relative antiviral protection is expressed as a percentage of total protection in VSV-infected organoids or (B) as the EC90 corresponding to the concentration of type I IFN (β) or type III IFN (λ1−3) resulting in 90% inhibition (10% infection) of viral replication. (C-D) Intestinal organoids were treated with type I IFN (β) (2,000 RU/mL equivalent 0.33 nM) or type III IFN (λ1−3) (100ng/mL each or total 300 ng/mL equivalent 13.7 nM) for different times prior to infection with VSV-Luc. Viral replication was assayed by measuring luciferase activity. (C) The relative VSV infection is expressed as the percentage of the luciferase activity present in VSV-infected organoids without IFN treatment (set to 100). (D) Pre-incubation time of type I IFN (β) or type III IFN (λ1−3) required to

1170 inhibit VSV infection to 10% (90% inhibition). (E-F) Same as (C-D), except
1171 intestinal organoids were treated at the indicated times post-infection with
1172 VSV-Luc. (F) Delayed-time post-infection for type I IFN (β) or type III IFN
1173 (λ1−3) to still inhibit VSV infection to 90% (10% inhibition). Data represent the
1174 mean values of two independent experiments with intestinal organoids
1175 generated from two different donors. Error bars indicate the SD. *<P.05, **P <
1176 0.01, ***P < 0.001, ns, not significant (unpaired t-test).
1177
1178 **Sup Fig 2. Kinetics of type I and type III IFN-mediated antiviral activities**
1179 **in human intestinal epithelial cells.** (A-B) T84 cells were pre-treated with
1180 the indicated concentrations of type I IFN (β) or type III IFN (λ1−3) for 2.5 h
1181 prior to infection with vesicular stomatitis virus (VSV) expressing Firefly
1182 luciferase (VSV-Luc) using a multiplicity of infection (MOI) of 1. Viral
1183 replication was assayed by measuring the luciferase activity. (A) The relative
1184 antiviral protection is expressed as a percentage of total protection in VSV-
1185 infected cells or (B) as the EC90 corresponding to the concentration of type I
1186 IFN (β) or type III IFN (λ1−3) resulting in 90% inhibition (10% infection) of viral
1187 replication. (C-D) T84 cells were treated with type I IFN (β) (2,000 RU/mL
1188 equivalent 0.33 nM) or type III IFN (λ1−3) (100ng/mL each or total 300 ng/mL
1189 equivalent 13.7 nM) for different times prior to infection with VSV-Luc. Viral
1190 replication was assayed by measuring luciferase activity. (C) The relative VSV
1191 infection is expressed as the percentage of the luciferase activity present in
1192 VSV-infected cells without IFN treatment (set to 100). (D) Pre-incubation time
1193 of type I IFN (β) or type III IFN (λ1−3) required to inhibit VSV infection to 10%
1194 (90% inhibition). (E-F) Same as (C-D), except T84 cells were treated at the

1195 indicated times post-infection with VSV-Luc. (F) Delayed-time post-infection
1196 for type I IFN (β) or type III IFN (λ1−3) to still inhibit VSV infection to 90%
1197 (10% inhibition). Data in (A–F) represent the mean values of three
1198 independent experiments. Error bars indicate the SD. *<P.05, **P < 0.01, ***P
1199 < 0.001, ****P < 0.0001, ns, not significant (unpaired t-test).
1200
1201 **Sup Fig 3. Type III IFNs have a lower transcriptional activity compared to**
1202 **type I IFNs in human intestinal epithelial cells.** (A-B) T84 cells were
1203 stimulated with indicated concentrations of type I (β) or III IFN (λ1−3) for
1204 different times and the transcript levels of the ISGs IFIT1 and Viperin were
1205 analyzed by qRT-PCR. Data are normalized to TBP and HPRT1 and are
1206 expressed relative to untreated cells at each time point. A representative
1207 experiment with technical triplicates, out of three independent experiments is
1208 shown. Mean values and SD are shown. (C-D) T84 cells were treated with
1209 type I IFN (β) (2,000 RU/mL equivalent 0.33 nM) or type III IFN (λ1−3) (300
1210 ng/mL equivalent 13.7 nM) for the indicated times and identification of the
1211 IFN-induced ISGs was performed by qRT-PCR. A total of 70 out of 132 ISGs
1212 tested were found to be significantly induced more than 2-fold compared with
1213 a baseline (mean of untreated controls at the particular time points) for at
1214 least one time point by at least one IFN treatment. Data are normalized to
1215 TBP and HPRT1. (C) Comparison of expression values (log2 (Fold Change))
1216 for all genes induced at the indicated times with type I IFN (β) versus type III
1217 IFN (λ1−3). Solid line indicates equivalent expression. (D) Hierarchical
1218 clustering analysis of these genes produced four distinct temporal expression
1219 patterns (Groups 1-4) based on the time-point of the maximum induction in

response to type I IFN (β) or type III IFN (λ1−3). Color codes have been used to visualize the induction peak per group. Gene expression heat map showing the genes clustered in their respective temporal expression patterns groups in response to type I IFN (β) or type III IFN (λ1−3). The genes per group are sorted in decreasing order on the basis of their fold change of expression in response to type I IFN (β) or type III IFN (λ1−3) and only showing the highest expressed values within the temporal groups omitting all other values for visualization.

Sup Fig 4. Comparison of the transcriptional response between wild-type IFNλ3 and high affinity H11-IFNλ3 variant. (A-D) T84 cells were stimulated with increasing concentrations of type III IFN (λ3) (WT-IFNλ3) or the high affinity IFNλ3 variant (H11-IFNλ3) for indicated times and the kinetic of expression of one representative ISG from each temporal expression groups 1-4 was analyzed by qRT-PCR, (left column) WT-IFNλ3, (right column) H11-IFNλ3 treated cells. Data are normalized to HPRT1 and are expressed relative to untreated cells at each time point. A representative experiment with technical triplicates. Mean values and SD are shown.

Sup Fig 5. **Analysis of mathematical model M3**. (A) Comparative simulation of type I and type III IFN receptor complex activation. Cellular concentration of the activated type I or type III IFN receptor complex, upon treatment with 0.1 nM of IFNs, are simulated using the calibrated model. (B) Profile likelihoods of model parameters. The uncertainty of the estimated model parameters is calculated using the profile likelihood method. The solid blue line is the

change in the weighted sum of squared residuals ($\Delta\chi^2$), the filled circle indicates the optimum parameter value, and the solid red line indicates the 95% threshold calculated using the χ2 distribution. (C) The 95% confidence bounds of type I or type III IFN receptor complex inactivation rate constants are calculated using the profile likelihood method. Our calculations show that the type III IFN receptor complex inactivation rate constant (k2) is significantly smaller than the corresponding rate constant for type I IFN receptor complex (k11). (D-E) The mathematical model shows the effect of IFNAR1 (D) and IFNLR1 (E) overexpression of up to 3-fold (3×IFNAR1 and 3×IFNLR1) on Viperin activation upon treatment with representative concentrations of type I IFN (β) (0.1 nM) or type III IFN (λ1−3) (13.7 nM), respectively.

Sup Fig 6. Expression levels of IFN receptors in T84 cells. (A) T84 wild-type cells, (B) T84 cells overexpressing rIFNAR1 (WT+rIFNAR1) and (C) T84 cells overexpressing rIFNLR1 (WT+rIFNLR1) were analyzed by qRT-PCR to quantify the transcript levels of IFNAR1, IFNAR2, IFNLR1 and IL10RB (IFNLR2). Data are normalized to HPRT1. The mean value obtained from three independent experiments is shown. Error bars indicate the SD. *<P.05, **P < 0.01, ***P < 0.001, ****P < 0.0001, ns, not significant (unpaired t-test).

Sup Fig 7. Type I and type III IFN receptors are functional when overexpressed into cells. (A-D) T84 IFNAR1-/- cells were rescued by stable expression of a cleavage resistant mutant of rIFNAR1 (see methods for details) (T84 IFNAR1-/- + rIFNAR1). (B-D) T84 IFNAR1-/-, T84 IFNAR1-/- + rIFNAR1 cells and control T84 cells scramble gRNA (SCR) were pre-treated

with type I IFN (β) (2,000 RU/mL equivalent 0.33 nM) or type III IFN (λ1−3) (300 ng/mL equivalent 13.7 nM). (B) 2.5 h post-treatment, T84 cells were infected with VSV-Luc (MOI = 1). Viral replication was assayed by measuring the luciferase activity. For each sample luciferase activity was measured in triplicates and is expressed as the percentage of the luciferase signal in VSV-infected cells without IFN treatment (set to 100) for each cell lines. (C) 1h post IFN treatment, IFN signaling was measured by immunoblotting for pSTAT1 Y701. Actin was used as a loading control. A representative immunoblot out of three independent experiments is shown. (D) same as (B), except that induction of IFN-stimulated genes was monitored by relative qRT-PCR quantification of IFIT1 and Viperin at the indicated times post-IFN treatment. (E-H) same as (A-D) except that T84 IFNLR1-/- were rescued by stable expression of a cleavage resistant mutant of rIFNLR1 (T84 IFNLR1-/- + rIFNLR1). Data were normalized to HPRT1 and are expressed relative to untreated cells of each time point. The mean value obtained from three independent experiments is shown. Error bars indicate the SD.

Sup Fig 8. Establishment of an antiviral state in cells overexpressing the IFN receptors and treated with IFNs. (A-H) Wild-type T84 cells were transduced with rIFNAR1 or rIFNLR1 to create stable lines overexpressing either receptor. (A-D) T84 wild-type cells (WT) and T84 cells overexpressing the IFNAR1 (WT+rIFNAR1) were treated with (A-B) type I IFN (β) (2,000 RU/mL equivalent 0.33 nM) or (C-D) type III IFN (λ1−3) (100ng/mL each =300 ng/mL equivalent 13.7 nM) at the indicated times (A, C) prior to infection or (B, D) post infection with VSV-Luc. Viral replication was assayed by measuring

the luciferase activity. The time necessary to confer IECs an antiviral state was addressed by measuring the impact of IFN treatment on viral replication. For each sample luciferase activity was measured in triplicates and is expressed relative to VSV-infected cells without IFN treatment (set to 100). (E-H) same as (A-D), but T84 wild-type cells (WT) and T84 cells overexpressing the IFNLR1 (WT+rIFNLR1) were treated with (E-F) type I IFN (β) (2,000 RU/mL equivalent 0.33 nM) or (G-H) type III IFN (λ1−3) (100ng/mL each =300 ng/mL equivalent 13.7 nM) at the indicated times (E, G) prior to infection or (F, H) post infection with VSV-Luc. Data represent the mean values of three independent experiments. Error bars indicate the SD. *<P.05, **P < 0.01, ns, not significant (unpaired t-test).

Sup Fig 9. Expression kinetics of ISGs are independent of the IFN receptor levels. (A-B) Wild-type T84 cells were transduced with rIFNAR1 or rIFNLR1 to create stable lines overexpressing either receptors. (A) T84 wild-type cells (WT) and T84 cells overexpressing the IFNAR1 (WT+rIFNAR1) were treated with increasing concentrations of type I IFN (β) for the indicated times and the expression kinetics of the ISG VIPERIN were analyzed by qRT-PCR. Data are normalized to HPRT1 and are expressed relative to untreated cells at each time point. (B) Same as (A), except T84 cells overexpressing the IFNLR1 (WT+IFNLR1) were used and treated with increasing concentrations of type III IFN (λ1−3). A representative experiment with technical triplicates, out of three independent experiments is shown. Mean values and SD are shown. (C-D) The mathematical model predicts the effect of IFNAR1 and IFNLR1 overexpression on Viperin activation upon treatment with different

concentrations of type I IFN (β) and type III IFN (λ1−3). The IFNAR1 and IFNLR1 levels were increased ~2.6 and ~1.5 fold, respectively, while all other parameters were held constant. The solid lines are the best fits and the shaded areas are 95% confidence intervals. (D) The mathematical model correctly predicts the IFNAR1 versus IFNLR1 overexpression, measured experimentally by qRT-PCR.

Sup Table 1. List of primers used in predesigned 384 well assay qRT-PCR. For the gene expression analysis of interferon stimulated genes (ISGs), qRT-PCR was performed using a predesigned 384-well assay of type I IFN response assaying the expression of ISGs. The Reference Sequence (RefSeq) accession number is provided for each ISG tested.

Sup Table 2. List of primer sequences used for qRT-PCR analysis. The expression of additional ISGs, transcriptional factors and housekeeping genes was analyzed by qRT-PCR with the primer sets shown in this table.

Sup Table 3. Mathematical formulation of the model. The table lists all differential equations explaining the dynamics of different biological species in our model. Cell surface (Area) is calculated as, Area = $(36\cdot\pi)^{1/3}\cdot V_{cell}^{2/3}$. Cell volume ($V_{cell}$) is assumed equal to 2×10^{-9} Liter. Brackets [ ] indicate the concentration of the respective biological species.

Sup Table 4. State variables and initial values. Biological species considered in the model (state variables) and their initial values are listed in the table.

Sup Table 5. Estimated parameter values. The estimated value of the model free parameters, their profile-likelihood based confidence bound and their dimensions are explained in the table. All reaction rate constants of the model, k_1-k_9, are practically identifiable.

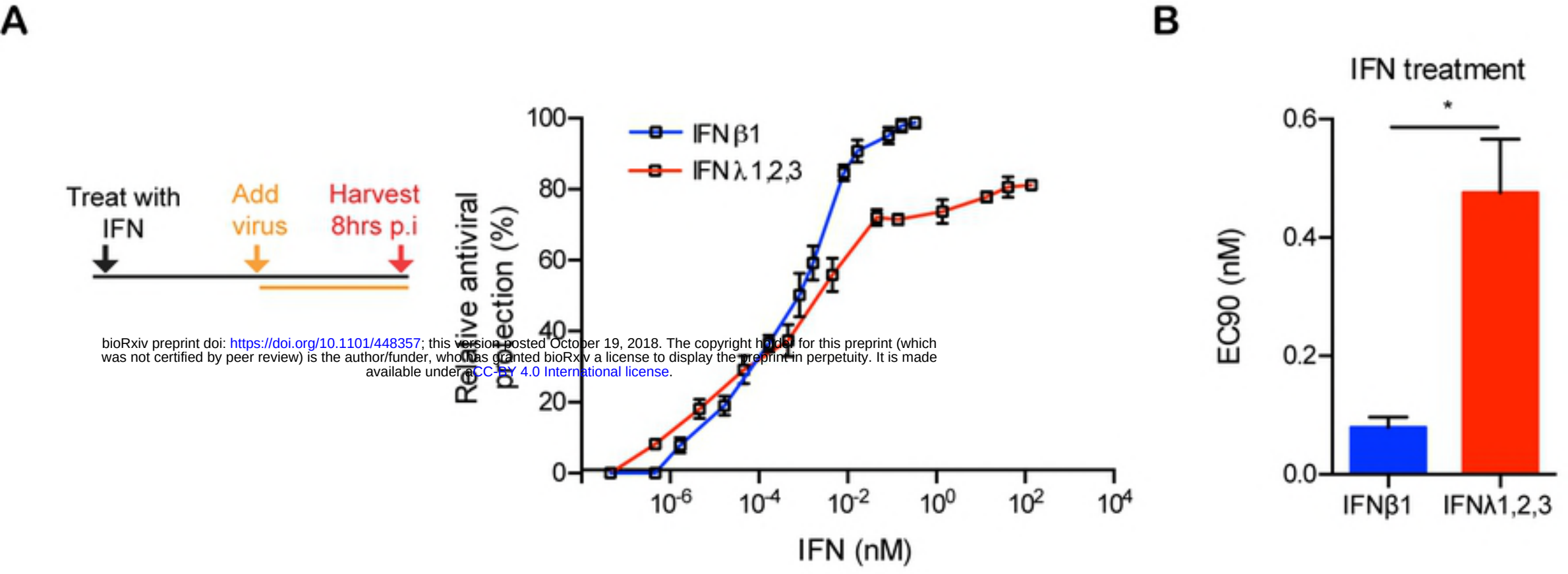

Fig1.tiff

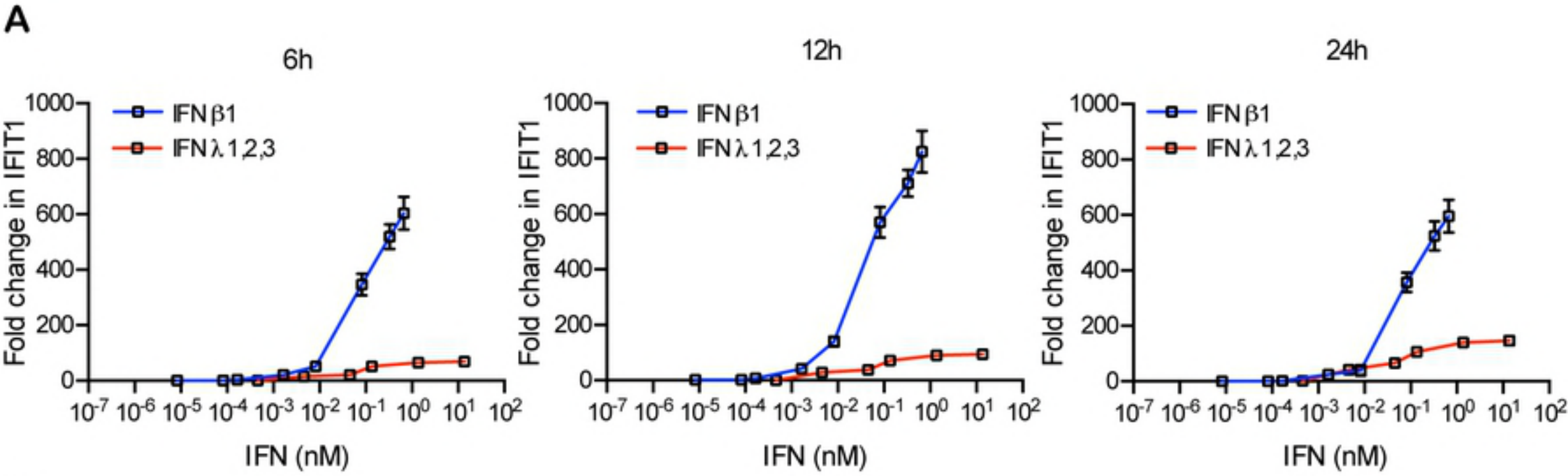

Fig2.tiff

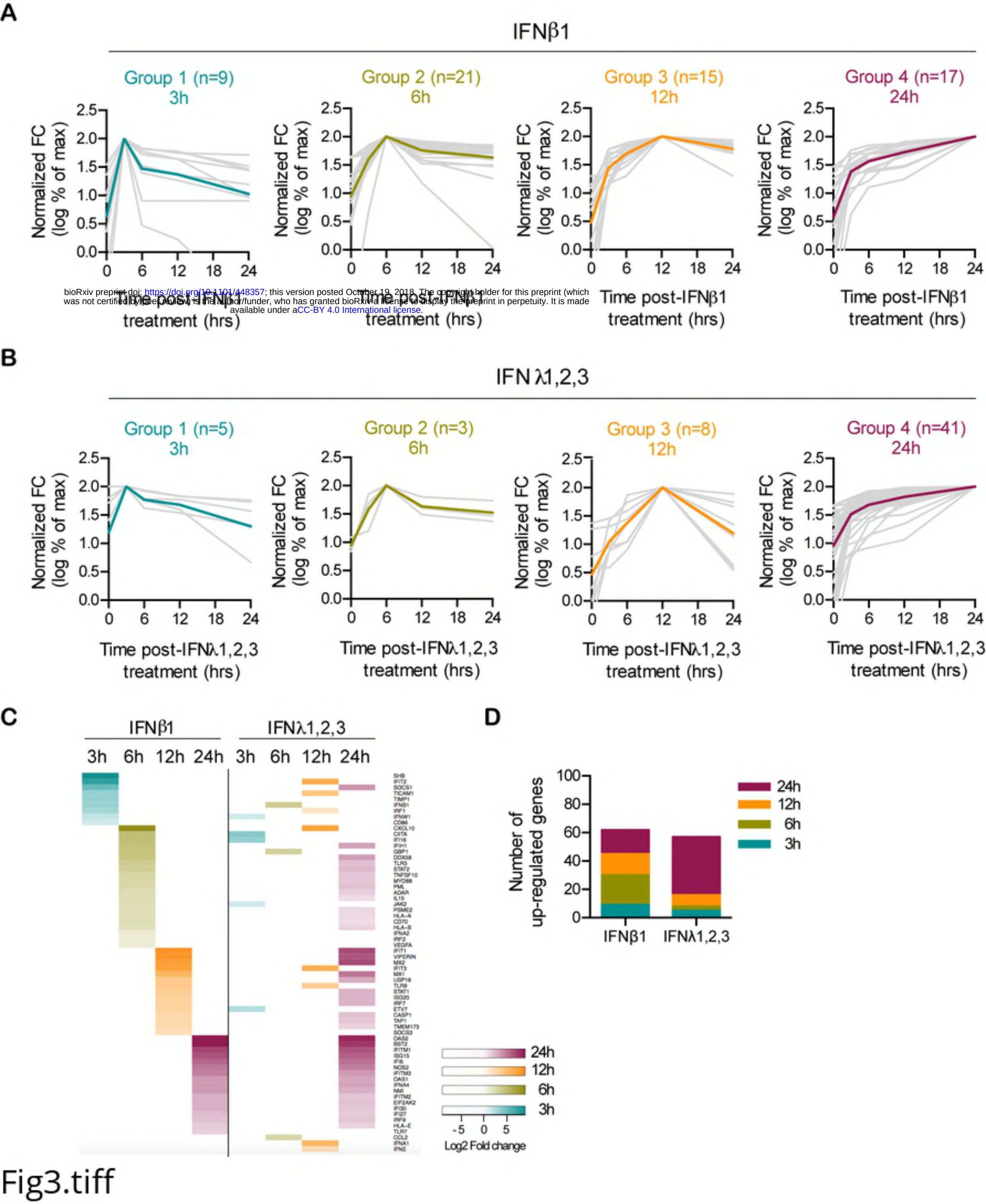

Fig3.tiff

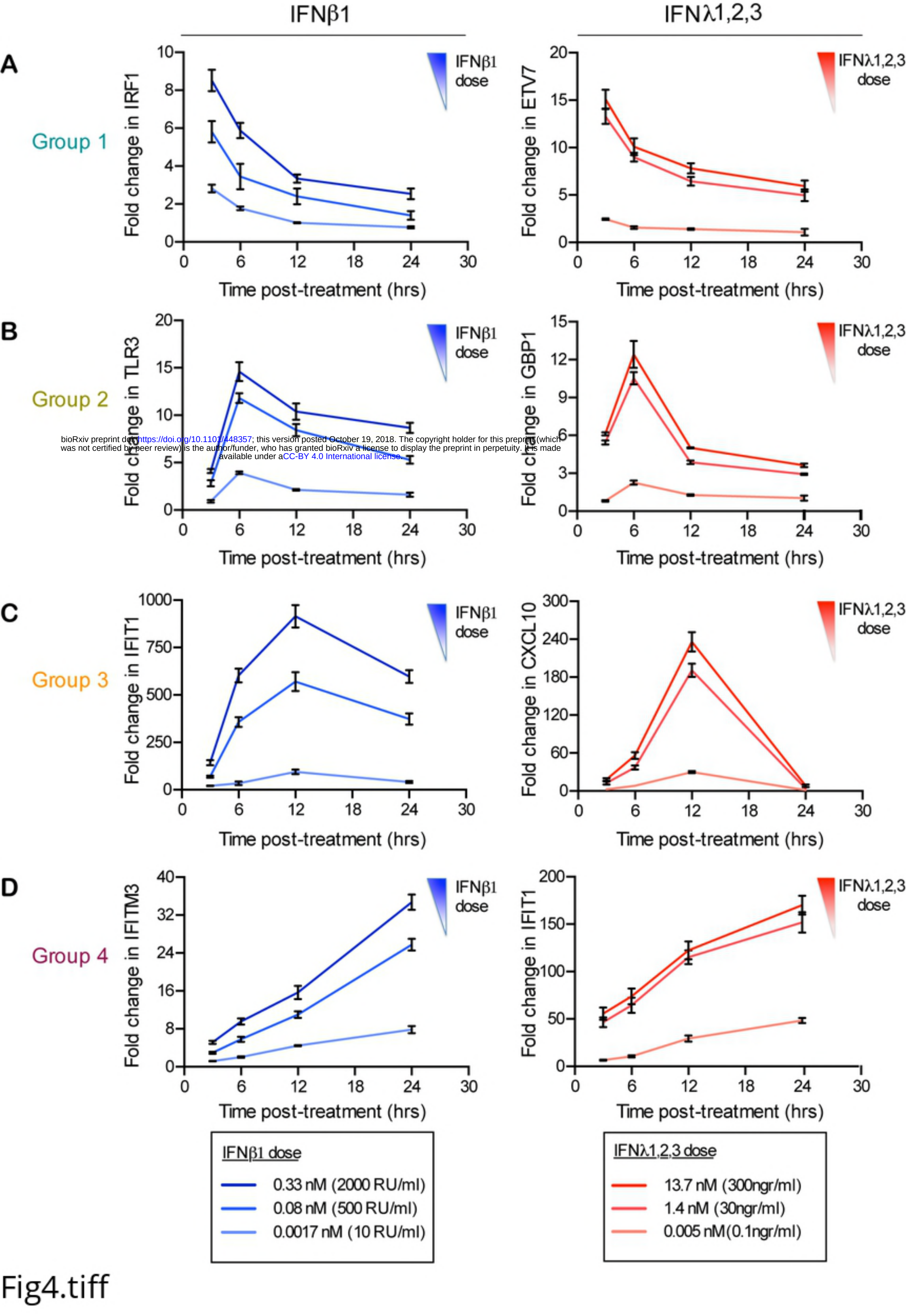

Fig4.tiff

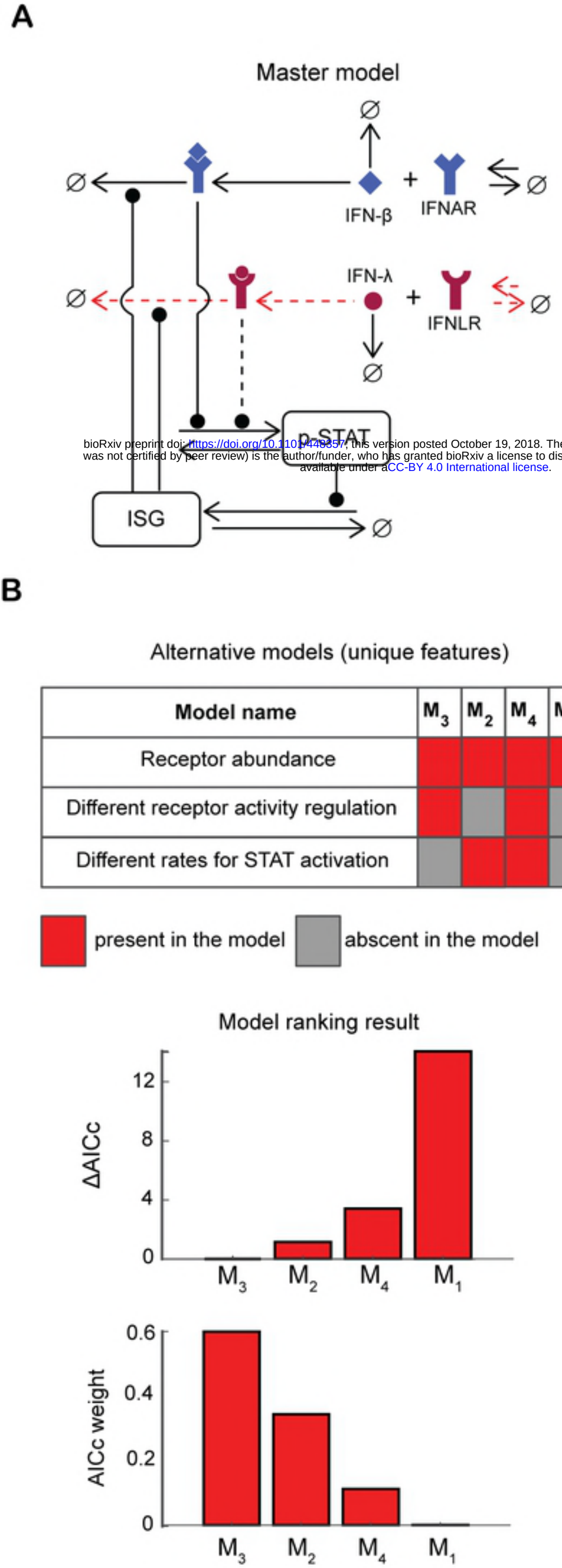

Fig5.tiff

Fig6.tiff

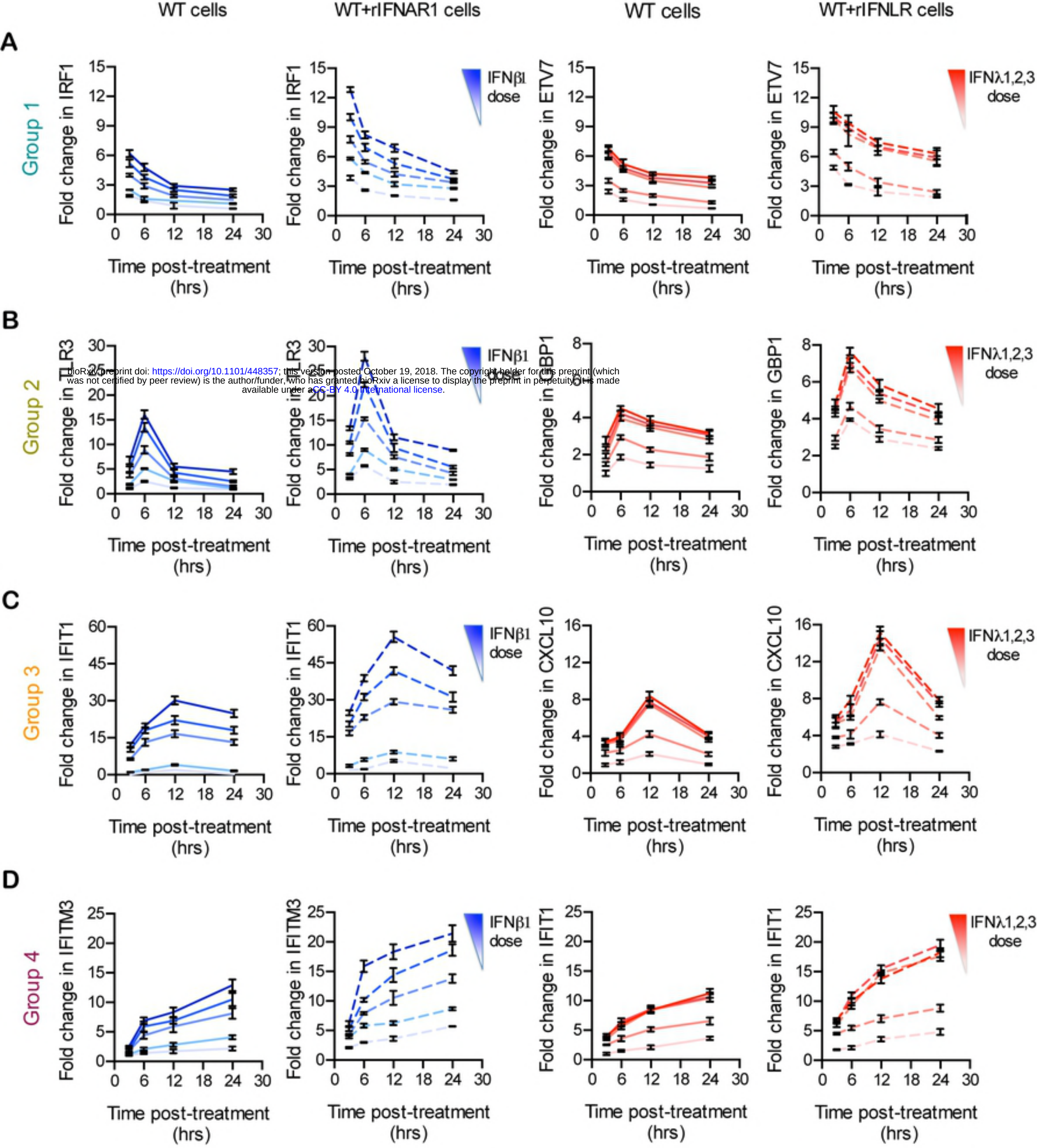

Fig7.tiff

A

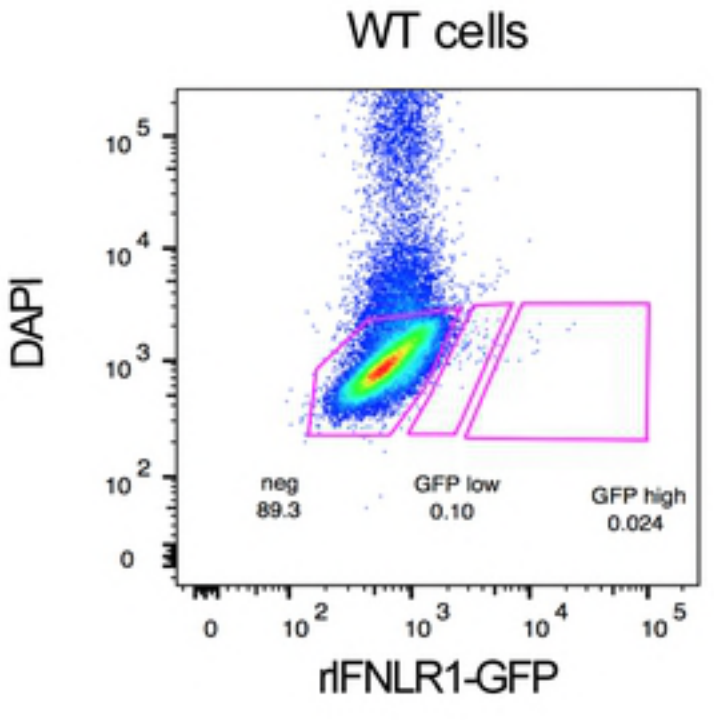

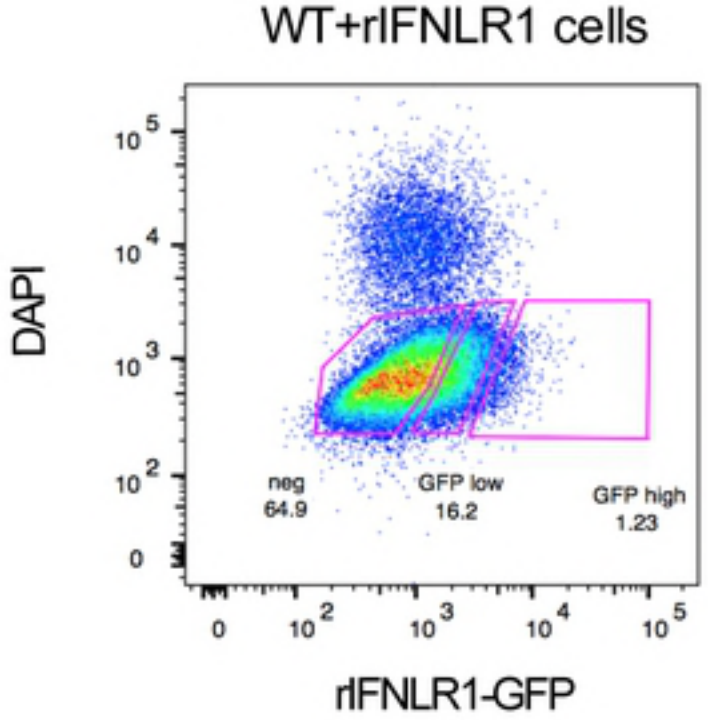

B

Group 1

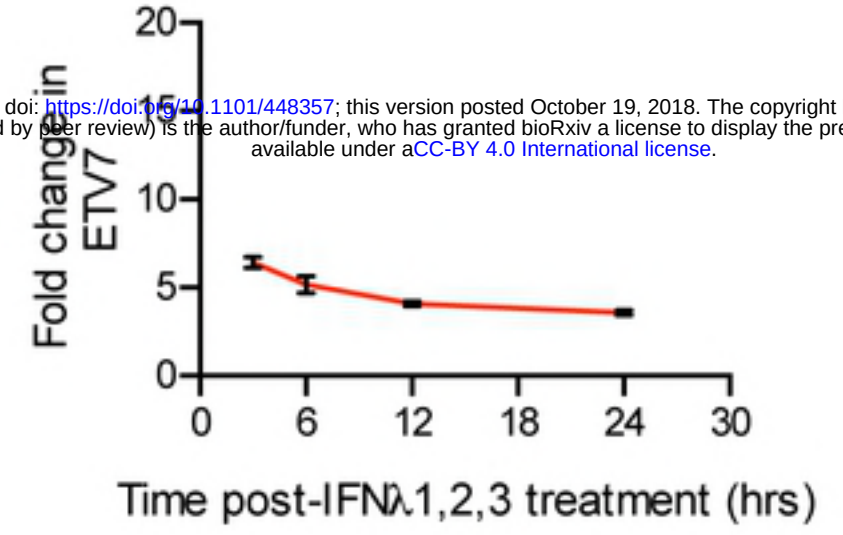

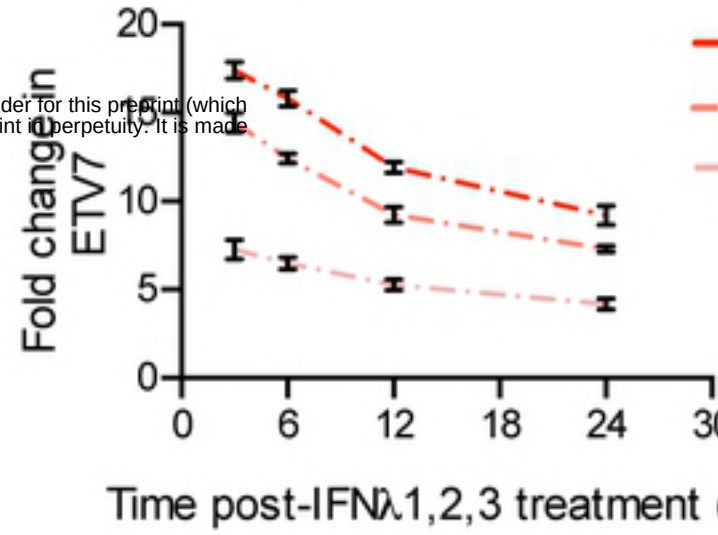

Group 2

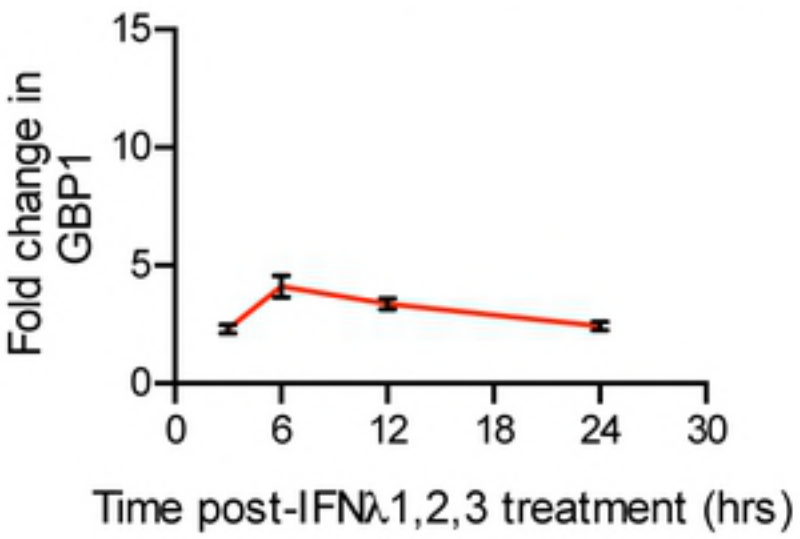

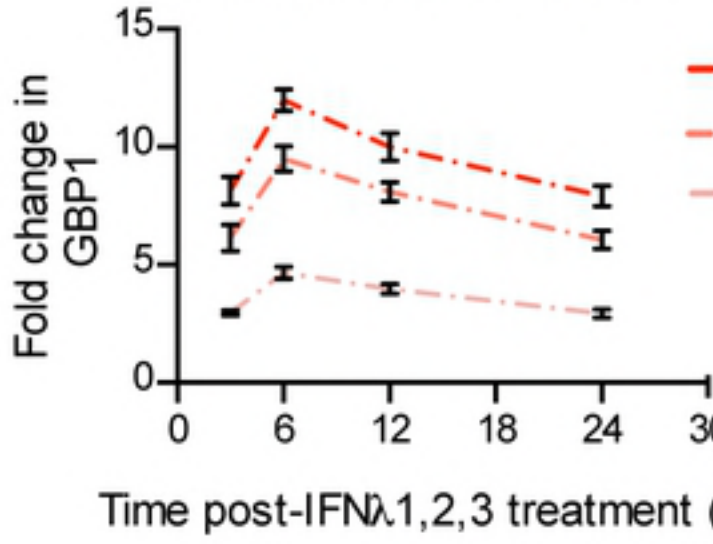

Group 3

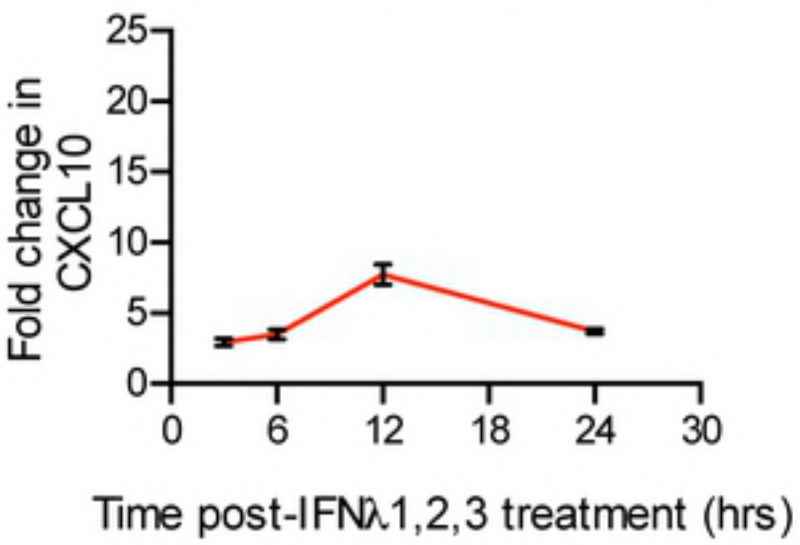

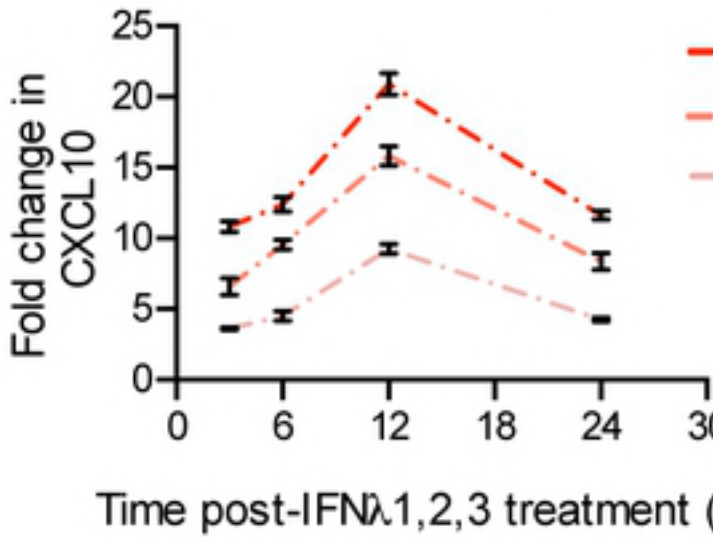

Group 4

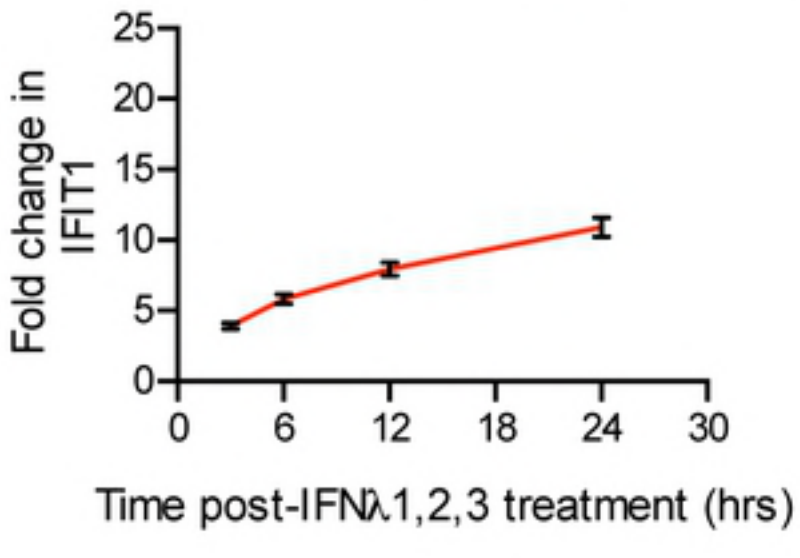

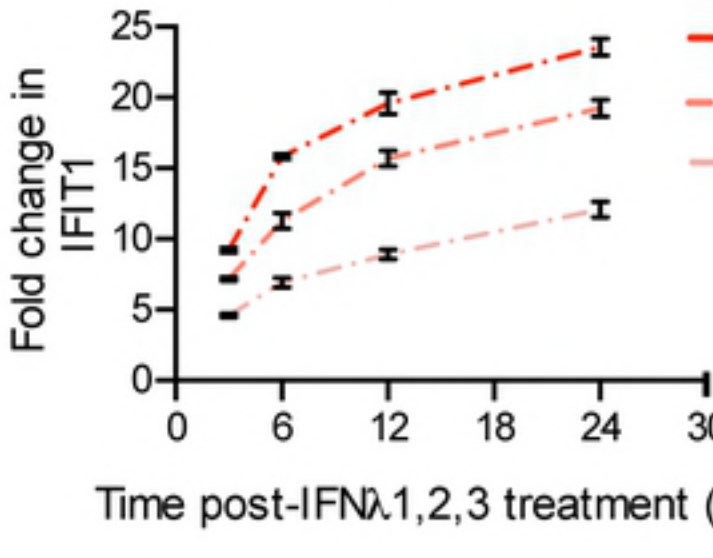

Fig8.tiff